Journal of Experimental Psychology:
Human Perception and Performance
2000, Vol. 26, No. 3, 1106–1132

0096-1523/00/$5.00 DOI: 10.1037//0096-1523.26.3.1106

From Vision to Action: Experiments and Models of Steering Control During Driving

Ellen C. Hildreth
Wellesley College

Jack M. H. Beusmans
Astra Research Center Boston, Inc.

Erwin R. Boer
Nissan Cambridge Basic Research

Constance S. Royden
Wellesley College

Experienced drivers performed simple steering maneuvers in the absence of continuous visual input. Experiments conducted in a driving simulator assessed drivers' performance of lane corrections during brief visual occlusion and examined the visual cues that guide steering. The dependence of steering behavior on heading, speed, and lateral position at the start of the maneuver was measured. Drivers adjusted steering amplitude with heading and performed the maneuver more rapidly at higher speeds. These dependencies were unaffected by a 1.5-s visual occlusion at the start of the maneuver. Longer occlusions resulted in severe performance degradation. Two steering control models were developed to account for these findings. In the 1st, steering actions were coupled to perceptual variables such as lateral position and heading. In the 2nd, drivers pursued a virtual target in the scene. Both models yielded behavior that closely matches that of human drivers.

When driving in natural conditions, one's attention is frequently drawn away from the steering task for short periods of time, often resulting in a reduction of visual input. For example, when a driver is in the process of reading the instrument panel or a road sign, adjusting the radio, or looking over his or her shoulder to prepare for a lane change, visual input in the direction ahead of the car is reduced and the driver's attention is diverted away from the steering task. During such times, steering must continue with minimal peripheral visual input or with a complete loss of relevant visual feedback. Driving is such a highly learned and generally low bandwidth motor skill that these momentary losses usually do not impair performance.

Most models for steering control proposed for human drivers and used to control autonomous vehicles assume that visual feedback is available for continuous error correction or monitoring (e.g., Donges, 1978; Groen, Hirose, & Thorpe, 1993; Iyengar & Elfes, 1991; Kanade, Groen, & Herzberger, 1989; Masaki, 1992; McRuer, Allen, Weir, & Klein, 1977; Modjtahedzadeh & Hess, 1993). From visual input, information about the vehicle and its relation to the road is continually evaluated and compared with a desired vehicle state. In many models, a desired state is defined at some future time and compared with a predicted vehicle state that would be achieved if the current steering action were maintained. The difference between these desired and predicted future states is used to make immediate steering corrections.

As a consequence of the need to coordinate many tasks during driving, human steering control cannot rely on the availability of a rich and continuous stream of visual input to guide steering at every moment. Drivers often must initiate appropriate steering actions and execute them briefly in the absence of error correction, while their attention is diverted to another task or while visual input is reduced. Even when attending to the steering task and the visual scene ahead of the car, the driver may execute an extended steering trajectory without making corrective adjustments if he or she is satisfied with the anticipated future state of the vehicle. Any viable model of human steering control must provide a plausible account of how and when drivers initiate appropriate extended steering actions and how they maintain effective control in the absence of continuous visual feedback.

Several empirical questions arise from these requirements for the models. How well do drivers execute steering maneuvers during visual occlusion, and what is the limit beyond which occlusion causes serious degradation in performance? What visual information guides steering when continuous visual input is available? How are appropriate steering actions initiated and maintained during the loss of visual input? What internal representation of information does the driver use to control steering? To address these questions, we conducted experiments in which experienced drivers executed a simple steering maneuver in a fixed-base driving simulator. The task involved a lane correction. We systematically varied the visual information available at the start of the steering maneuver and compared steering performance with constant visual feedback with performance during the temporary re-

Ellen C. Hildreth and Constance S. Royden, Department of Computer Science, Wellesley College; Jack M. H. Beusmans, Astra Research Center Boston, Inc., Boston, Massachusetts; Erwin R. Boer, Nissan Cambridge Basic Research, Cambridge, Massachusetts.

This work was conducted at Cambridge Basic Research and was sponsored by Nissan Research and Development, Inc. This work was also supported by National Science Foundation Grant SBR-930126.

Correspondence concerning this article should be addressed to Ellen C. Hildreth, Department of Computer Science, Wellesley College, 126 Central Street, Wellesley, Massachusetts 02481-8203. Electronic mail may be sent to ehildreth@wellesley.edu.

moval of visual input. To examine the limit of driver performance during occlusion, we varied the duration of the occlusion.

The experimental results are discussed in the context of two fundamentally different models of steering control. The first embodies an approach from control theory, in which drivers continually adjust steering to regulate the state of perceptual variables that are relevant to the task. In particular, we consider a proportional-derivative (PD) controller (Dorf & Bishop, 1995) that regulates the perceptual variables of lateral position and its first and second temporal derivatives. The second model assumes that during the execution of a lane correction, the driver continually steers the car toward a virtual target in the environment. This approach was motivated by a model of curve negotiation proposed by Boer (1996), in which the driver steers toward the tangent point on the inner lane boundary of a curve.

Experimental data were used to guide the development of the models and to evaluate their suitability for human steering control. In the experiments, we manipulated a set of perceptual variables and examined their effect on steering performance. The particular perceptual variables chosen may not directly control human steering, but any viable model must respond to changes in these variables in the same way as human drivers. The models were formulated to yield steering actions with similar dependencies on the perceptual variables and to match the detailed shape of human steering trajectories. The experiments revealed significant differences in steering behavior across drivers. Both models capture these differences through changes in model coefficients, shedding light on the aspects of steering control that can lead to driver differences. Finally, we examined performance during visual occlusion, establishing performance limits that must be achieved by any viable model in this situation. We considered how these two models can continue control during visual occlusion. In particular, we examined whether this control could be based on a continuous extrapolation of the perceptual information used to guide steering, without planning an extended steering trajectory in advance. Both models exhibit steering behavior similar to that of human drivers. The target model offers a more intuitive account of the underlying basis for human driving behavior and extends more easily to other steering tasks, such as lane changes and curve negotiation.

In the next section, we summarize previous empirical work that demonstrates that drivers can execute simple steering maneuvers successfully in the absence of constant visual feedback and briefly review previous approaches to the design of steering control models. We then present the results of our driving experiments that examine steering performance during a lane correction. The two models of steering control are then presented in detail, and the results of the experimental work are further analyzed and discussed in the context of these models. We conclude with a brief discussion of the broader implications of our work for the coordination of multiple tasks during driving and for visuomotor integration.

Background

Driving Performance Under Visual Occlusion: Previous Empirical Work

Godthelp (1985) explored drivers' ability to make lane changes, both in a driving simulator and in a real car on an open road. The experiments compared performance with constant visual feedback with the performance achieved when visual input is removed briefly at the start of the lane change. For the experiments using a driving simulator, visual occlusion lasted for 1 s; in the experiments with a real car, this period was extended to 3 s. Drivers executed the lane change well under constant visual feedback and when visual input was temporarily removed at the start of the maneuver. The variability of the steering wheel activity and spatial path of the car was slightly higher under occlusion, and there was sometimes a small overshoot of the target lane position in this case. On average, however, drivers performed the task well in both conditions.

A second study involved steering around a curve of constant curvature (Godthelp, 1986). These experiments were conducted with a real car driven at constant speed on a road with curves of different curvature. Performance with constant visual feedback was compared with the performance achieved during occlusion that began 0.5 s before the start of the curve and lasted for 1.5 s. The steering angle required to negotiate a curve successfully increased with road curvature and speed. By occluding the road upon curve entry, Godthelp examined whether the steering change can be executed successfully without visual feedback and whether it is adjusted correctly with road curvature and speed. The results showed little degradation in performance under occlusion, with drivers adjusting their steering correctly with changing conditions. This suggests that drivers can initiate an extended steering trajectory that is determined by the current conditions of the vehicle and road.

Cavallo, Brun-Dei, Laya, and Neboit (1988) examined drivers' ability to negotiate curves when occlusion is introduced at different positions. They compared performance under constant visual feedback with that obtained when vision was briefly occluded, beginning 2 s before curve entry or at the start, the middle, or near the end of the curve. When occlusion began 2 s before curve entry, drivers started the steering change at the same moment as they did under constant visual feedback and turned the wheel in a single smooth movement to the correct angle needed to negotiate the curve. When occlusion began at the middle of the curve, drivers underestimated the appropriate time to realign the steering wheel to pull out of the curve but correctly rotated the wheel by the amount needed to straighten the car at the end of the curve. Cavallo et al. (1988) noted that drivers cannot drive the entire curve under occlusion, suggesting that some visual feedback is required to correct for accumulated errors in lane position during the maneuver.

From these studies, it appears that experienced drivers can execute simple steering maneuvers without constant error correction based on continuous visual feedback. The initiation of appropriate extended maneuvers appears to take into account visually derived information about the car and its surroundings. Using a driving simulator to control the visual conditions more carefully, we explored in our experiments the visual information used to initiate an extended steering maneuver and the limits of steering performance under occlusion.

Models of Steering Control

Some models of steering control have been developed to guide autonomous vehicles or mobile robots (see, e.g., Groen et al., 1993; Iyengar & Elfes, 1991; Kanade et al., 1989; Masaki, 1992;

Thorpe, 1990); others are aimed at explaining human driving behavior (see, e.g., Boer, 1996; Donges, 1978; Levison & Cramer, 1995; McRuer et al., 1977; Modjtahedzadeh & Hess, 1993; Reid, Solowka, & Billing, 1981). The design of an automatic controller to perform a driving task and formulation of a model that characterizes human performance of this task are often based on different criteria. Issues of computational efficiency, vehicle stability, and robustness to disturbances and noise are especially important in the design of automatic controllers. When trying to model the human driver, we encounter modeling constraints in issues such as the perceptual plausibility of the control input, limitations imposed by the motor system, and the need to coordinate multiple tasks during driving. The existence of empirical data on human driver performance provides a rigorous basis for the identification and evaluation of models of human steering control. Although some automatic controllers are suitable for modeling human drivers, we focus on controllers that have been developed specifically to explain human steering behavior. We only consider models of lateral control during lane keeping and do not address longitudinal control.

Models for human steering control can be divided into three classes: pursuit controllers, preview controllers, and optimal controllers. *Pursuit controllers* regulate instantaneously measured perceptual variables, such as lateral position, heading, or target bearing, to desired values that are usually zero. These controllers react to the currently perceived error in these variables; they do not use prediction of their future state and so do not embody any planning of an extended steering action. The act of keeping straight in a lane (referred to as *lane keeping* hereinafter) has been modeled using pursuit control (Hess & Modjtahedzadeh, 1990; McRuer & Weir, 1969; Reid et al., 1981). *Preview controllers* regulate variables about some future reference. This requires an internal model to predict the future state of perceptual variables, given the current state of the vehicle. The predicted deviation from the desired state is used in control. These controllers have a weak notion of planning because they can use their internal model of the vehicle's response to steering input together with their predictive abilities to continue control without constant input, up to the preview horizon. In essence, they apply pursuit control on a predicted error (Donges, 1978; McRuer et al., 1977; Modjtahedzadeh & Hess, 1993). *Optimal controllers* fully exploit planning. These models compute a complete control profile up to some (receding) preview horizon by minimizing an explicit cost function. This function includes terms that depend on predicted errors in perceptual variables as well as terms related to driver comfort, such as smoothness of control. The resulting steering profile can be executed successfully without sensory input as long as the noise in the perceived input is low, uncertainty in the internal model is minimal, and accuracy in control execution is high. These controllers are often used to compute a desired reference track through an obstacle course or to follow an externally specified reference track such as the center of a lane on a winding road. Optimal controllers have been used to model lane keeping in human drivers (Levison & Cramer, 1995).

For the models introduced in this article, steering control under constant visual feedback is modeled as pursuit control. Some of the predictive capability of preview controllers is added to model how drivers continue control during visual occlusion. We examined pursuit controllers first because of their simplicity and found that such models adequately account for human steering behavior under continuous visual guidance. Given the use of straight roads in our experiments, knowledge of the reference that is used for pursuit or preview control is accurate and implicit, which renders the two approaches similar. Some discussion of the application of optimal control to our driving task can be found in Boer, Hildreth, and Goodrich (1998).

Experiments: Steering Control With and Without Visual Feedback

Experienced drivers performed a simple steering maneuver in a fixed-base driving simulator composed of the frontal two thirds of a Nissan 240SX convertible, coupled to a computer-controlled, wide-field-of-view display of a simulated driving scene (Beusmans & Rensink, 1995). The steering task involved a lane correction, in which drivers steered the car to correct for an initial deviation in heading and lateral position from a desired state. We explored how well drivers execute this maneuver with constant visual feedback and with the temporary loss of visual input for different lengths of time. We systematically varied the speed, heading, and lateral position of the car at the start of the maneuver and examined the effect of these manipulations on quantitative aspects of drivers' steering actions, such as their amplitude and time course. Correlation between the initial visual conditions and subsequent steering behavior provides insight into the information used to guide steering. In this section, we describe the basic empirical results and provide statistical analyses of observed trends in the data. In the next section, we further analyze the data in the context of the two models that we develop in detail.

General Method

Participants. Six experienced drivers, ranging in age between 20 and 40 years old, with normal or corrected-to-normal vision, served as participants for all of the experiments. The participants included 3 of the authors and 3 drivers who were naive about the purpose of the experiments. The authors showed somewhat higher consistency in their steering data, in part owing to more experience with the driving simulator. The basic trends in the data, however, were observed across all drivers.

Stimuli and task. The steering task is illustrated in Figure 1. Figure 1A shows a bird's eye view of the driving situation, and Figure 1B shows a schematic drawing of the scene viewed by the driver. An Indigo (Model No. CMNB007A Silicon Graphics, Inc., Mountain View, CA) workstation was used to generate the graphics that were projected onto a wall 3.5 m in front of the driver by a Barco 800G system (Model No. 800B, Kuurne, Belgium). The display subtended 60° horizontally and 40° vertically and continually changed at an average rate of 20 frames per second (varying between 19 and 21), in correspondence with the movement of the car. The surface of the road was dark gray, the sky was dark blue, and the surrounding ground was green. Along the center of the road was a thick, continuous white line. Each lane was 4 m wide. Trees along the side of the road added visual texture to aid the driver in assessing the 3-D motion of the car. The trees were shaped like cones, with a textured brown surface color that was shaded to convey their 3-D shape. The trees had a random height varying between 12 and 28 m and were randomly positioned. The average distance between trees was 20 m along the direction of the road, and the distance of each tree from the edge of the road varied from 3.5 to 8.5 m. Drivers performed free eye movements.

The driving simulator provided auditory feedback regarding car speed, in the form of increased engine noise with increased speed, and tactile feedback through the torque in the steering wheel. Because of the fixed-base nature of the simulator, it did not provide the vestibular feedback that

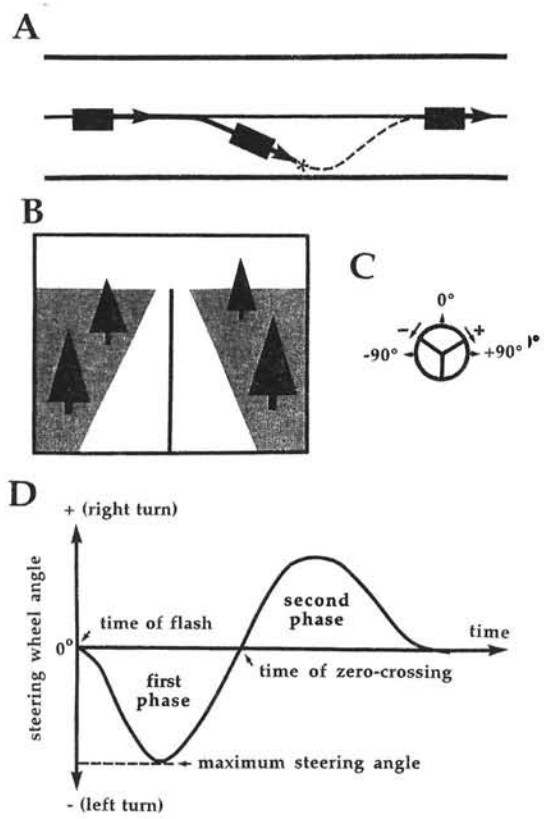

Figure 1. The basic steering task and display of data. A: Bird's eye view of the road and the path of the car during a trial of the experiment. The car first moves automatically down the road, centered on the midline, and then turns to move at an oblique heading (solid curve). After a flash of the display (asterisk), the driver steers the car back to the midline (dashed curve). B: A schematic drawing of the scene viewed by the driver. C: Definition of steering wheel angles—the resting position is labeled 0°. Angles in the counterclockwise direction are negative, whereas those in the clockwise direction are positive. D: A time sequence of steering angles that successfully completes this task.

drivers normally experience during accelerations, decelerations, and turns. This conflict between visual and vestibular input may have the capacity to cause drivers to underestimate speed and the effect of steering actions on the movement of the car, which may lead to more aggressive steering actions that would yield excessive lateral acceleration under normal driving conditions. However, we assume that although perceptual input may be distorted as a result of the use of a driving simulator and the vestibular conflict, drivers still use the same basic visual cues to adjust their steering actions that are used in normal driving. Our data analysis focuses on the relative effects of cue manipulation, rather than on the absolute properties of the steering responses.

During each trial, the car initially moved straight down the center of the road, with the driver centered on the midline. After 4 s, the car turned and followed a straight path at a new constant heading (the direction of motion of the driver and the direction the car was pointing were the same). During this initial movement, shown by the solid path in Figure 1A, drivers were asked to keep the steering wheel stationary in its upright position to assure that the car remained on this specified path. A few seconds later, the display quickly flashed off and on over two adjacent frames to signal the driver to initiate a corrective maneuver. The driver's task was to return the car to the midline so that it was again moving straight down the center of the road. The dashed curve in Figure 1A shows a sample path that the driver might follow. Throughout each trial, the car moved at a constant speed that the driver could not change. We gave no explicit instructions on how to steer back to the center line. We did not indicate, for example, that the maneuver should be completed as fast as possible, and there were no markers along the road to constrain the driver's path. We simply asked the driver to execute the maneuver in whatever way seemed most natural. Thus, the steering task was highly unconstrained; in principle, many steering trajectories could have successfully completed the task.

The experiments were conducted under two main conditions. In one case, there was constant visual feedback throughout the steering maneuver. In the second case, the screen was blank for a short time during the maneuver. The blank period began 0.5 s after the flash occurred to signal the driver to start the maneuver. For Experiments 1–3, the screen was blank for 1.5 s. In Experiment 4, the duration of the blank period was varied. While visual input was removed, the driver was expected to continue to execute the maneuver in a natural way, and when visual input returned, the visual scene was in a state that took into account the driver's steering actions during the blank period. The use of a 0.5-s delay between the flash and start of the blank period was based on pilot data that indicated that this amount of time is needed for drivers to assess the visual situation and to initiate a motor response.

Under natural conditions, drivers simultaneously control steering and speed. We limited the driver's task to steering control alone, with the hope that this would result in a more consistent relationship between visual input and performance. Adding speed control would permit a greater range of actions that could successfully complete the task, which could lead to greater variability even within individual drivers. Furthermore, while the combined control of steering and speed may be more complex in natural driving conditions, performance may still be influenced by the same visual cues used in steering control alone. In our experiments, we examined the effect of speed, to some extent, by varying speed across trials in Experiment 2. Given the range of speeds and the small lateral deviations and heading deflections used in the experiments, we did not expect substantial adjustments of speed through braking to take place in the natural driving situation.

Procedure. In Experiments 1, 2, and 3, respectively, we systematically varied the heading, speed, and lateral position of the car at the time of the flash that signaled the driver to start the maneuver. These experiments were conducted in blocks of trials that held two of these properties constant and varied the third. The constant visual feedback and blank conditions were tested in separate blocks. Drivers were given a sequence of 10 practice trials before each block of test trials. The task itself was not difficult. The tasks conducted with the blank period were disconcerting at first, but drivers quickly became accustomed to the temporary loss of visual input during the 10 practice trials and subsequently performed the steering task with little difficulty.

Display of driver steering data. Much of the data are displayed as steering angle time sequences. Figure 1D shows a sample steering angle time sequence that could complete this maneuver. The initial resting position of the steering wheel that moves the car straight is defined as 0°. The wheel was in this resting position at the start of the maneuver. Steering angles to the left of this position are defined as negative, and angles to the right are positive, as shown in Figure 1C. In Figure 1D, time is shown on the horizontal axis, with 0 corresponding to the time of the flash. In this ideal steering profile, the steering angle begins to change immediately after the flash. Human drivers exhibit a delay of 400–500 ms before turning the steering wheel.

The steering angle profile is roughly sinusoidal. Because the car initially heads to the right of the midline, the steering wheel is first rotated to the left to turn the car around to point toward the midline. As the car approaches the midline, the steering wheel is rotated to the right to realign the car with the road. The wheel is returned to the 0° position when the driver is centered on the midline and driving straight. We refer to the negative and

positive phases of the steering profile as the first and second phases. Because the car initially moves at an oblique heading relative to the road, the two phases are not symmetric. Our analysis of the steering data refers to two properties labeled in Figure 1D. The first is the maximum steering angle to the left, during the first phase of the maneuver. The second is the first time at which the steering wheel passes through 0°, between the two phases.

Experiment 1: Driving Under Occlusion and the Effect of Heading

Procedure. In this experiment, the speed and lateral position of the car at the time of the flash were held constant, and its heading at this moment was varied over five values: 1.0°, 1.5°, 2.0°, 2.5° and 3.0° to the right of straight ahead. This experiment was conducted for two speeds: 20 and 25 m/s. The lateral position of the car at the time of the flash was 2.7 m to the right of the midline. The experiment was conducted in four blocks of 50 trials. Each block contained 10 trials for each of the five headings, presented in a random order, and contained trials for a single speed and one feedback condition (constant visual feedback or temporary blank period). Prior to each block of 50 trials, drivers performed 10 practice trials with two trials for each heading.

Results and discussion. Figure 2 shows sample results of individual trials for 4 of the 6 drivers for the case of constant visual feedback. The performance of these drivers was representative of the range observed. The four figure panels show steering angle time sequences for 10 trials, for the 4 drivers. The data are shown for the initial heading of 1.5° and speed of 20 m/s. Individual drivers executed this maneuver very consistently. The first phase of the maneuver varied little across trials, but variability increased during the second phase (quantitative measures are presented later). This was to be expected because the need to compensate for errors that accumulated during the first phase might have required a greater range of corrective maneuvers during the second phase.

Although each driver had a natural strategy for carrying out this maneuver that was common across all conditions, this strategy varied considerably across drivers. Driver 1 completed the first phase in about 2 s and reached a maximum steering angle to the left of about 40°. In contrast, Drivers 3 and 4 took roughly 4 s to complete the first phase and reached a maximum steering angle of only about 15°. The qualitative shape of the steering angle profiles also differed. For Drivers 1 and 2, the profile was sharply curved through the first phase, indicating that the steering wheel was constantly moving, sometimes at a high velocity. In contrast, Driver 4 turned the wheel quickly to the left but then paused for about 2 s before slowly returning the wheel to the 0° position. Variation between drivers may have been enhanced by the use of a driving simulator. In a real car, vestibular feedback may discourage the large, rapid steering changes seen in the data for Driver 1, although the lateral accelerations that would be produced here are within the range observed in normal driving. The variation across drivers reinforces the unconstrained nature of the steering task, for which drivers clearly adopt different solutions.

Evidence of corrective adjustments to the steering trajectory, possibly due to visual feedback, was first seen about 1–2 s after the start of the maneuver. The corrections typically took the form of momentary holds of the steering wheel in a fixed position and occasionally included brief oscillations superimposed on the general steering wheel movement pattern.

Figure 3 shows the same data for individual trials for the case in which a 1.5-s blank period occurred after the initiation of the

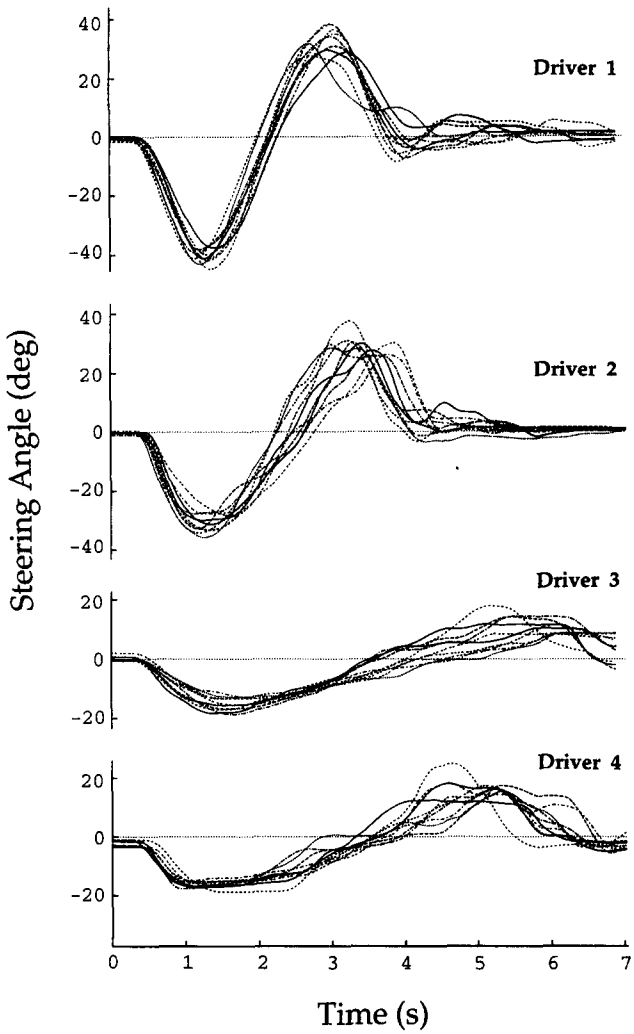

Figure 2. Data from individual trials for the constant feedback condition. The four panels show the steering angle time sequences for each of the 10 trials, for 4 different drivers. The heading prior to the flash was 1.5°, speed was 20 m/s, and lateral position was 2.7 m. Constant visual feedback was available throughout the trials.

maneuver. The extent of the blank period is highlighted on the horizontal axis of each graph. Data for the same initial conditions and drivers are shown in Figures 2 and 3. The data in Figure 3 suggest that drivers executed the maneuver in a way that was similar to the constant feedback condition, despite the temporary absence of visual input. For 3 of the 6 drivers, the first phase of the steering profile was complete or nearly complete during the blank period. For Drivers 3 and 4, it appears that their strategy was to turn the wheel to the left and then wait until visual feedback returned before continuing with the maneuver. Because drivers knew in advance that the blank would occur and how long it would last, they may have consciously adjusted their steering behavior to accommodate the blank period. Even in the constant feedback condition, however, Drivers 3 and 4 had a tendency to turn the wheel to the left and to wait before turning the wheel back to the right. In a later experiment, we varied the duration of the blank period to reduce its anticipatory effect on steering performance.

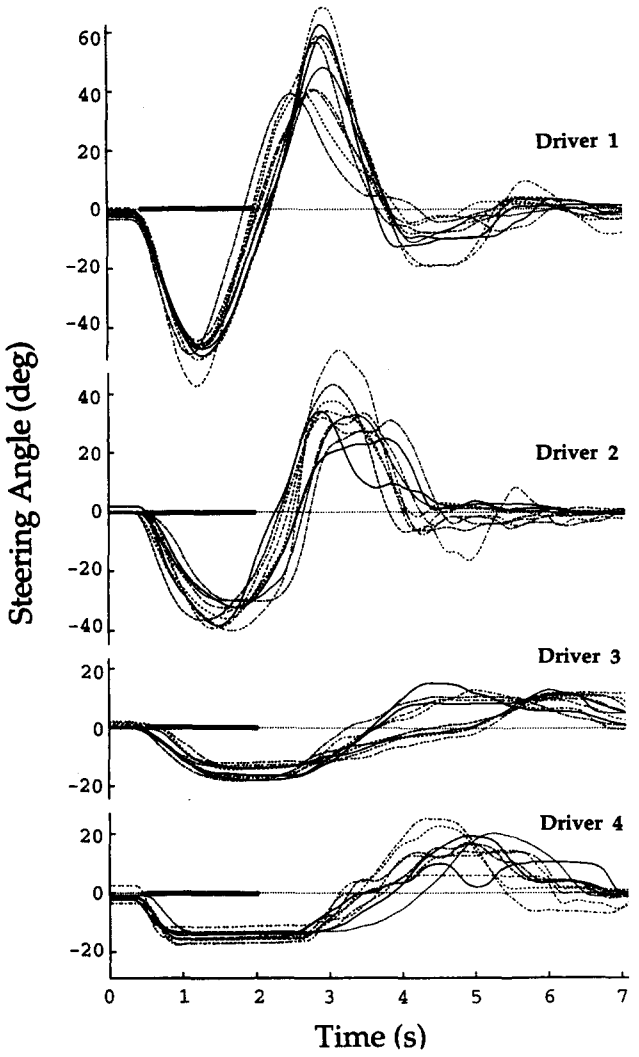

Figure 3. Data from individual trials for the blank condition. The four panels show the steering angle time sequences for each of the 10 trials, for 4 different drivers. The heading prior to the flash was 1.5°, speed was 20 m/s, and lateral position was 2.7 m. The screen was blank for 1.5 s, starting 0.5 s after the flash. The period of the blank is highlighted by a bold line on the horizontal axis of each graph.

After vision returned, there was a delay of about 0.5 s during which drivers reassessed their situation and initiated a response to the visual input. Drivers 3 and 4 maintained their constant steering angle to the left for about 0.5 s beyond the end of the blank period, which sometimes resulted in a large rotation of the car to the left. A large turn of the wheel to the right, sometimes seen as a high peak during the second phase, reflected a correction for this rotation. For Driver 2, corrective adjustments sometimes resulted in a broad, delayed peak during the second phase. The lack of a highly stereotyped pattern in the second phase of the steering profiles in both the constant feedback and blank conditions suggests that drivers corrected their steering as needed to complete the task successfully, given the highly variable error that accumulated during the first phase.

Figure 4 shows data from individual trials, in which the lateral position of the car is plotted as a function of the distance down the road. Lateral position was 0 m when the car was centered on the midline. We asked drivers to center themselves on the midline at the completion of the maneuver; in this final state, the lateral position of the car was 0.3 m. A distance down the road of 0 m corresponds to the position of the car at the time of the flash. (The scales on the two axes differ, so that lateral position is exaggerated relative to distance down the road.) The data in Figures 4A and 4B were obtained under constant visual feedback, whereas the data in Figures 4C and 4D were obtained for the blank condition. The screen was blank from about 10 to 40 m down the road, as shown by the bold line on the horizontal axes of the graphs in Figures 4C and 4D. The data in Figures 4A and 4C were obtained from Driver 1, whereas the data in Figures 4B and 4D were obtained from Driver 3. Driver 1 had a tendency to overshoot the midline when the blank screen was present. Overall, all drivers showed similar consistency in the path on the road that was followed, across the constant feedback and blank conditions (quantitative measures are presented later).

Two properties of the steering profile that capture the effect of the initial visual conditions and differences between drivers are its amplitude and duration. With regard to amplitude, we examine the maximum angle reached during the first phase. With regard to timing, a well-defined point is the time of the first *zero-crossing*—a time when the steering wheel passes through the 0° position between the two phases.

The primary effect of changes in the heading of the car at the start of the maneuver is adjustments in the amplitude of steering. Figure 5 shows mean steering angle data for Drivers 1 and 3, for the five headings tested for the 25 m/s speed condition and for the constant visual feedback condition. The performance of these drivers is representative of the range observed across all 6 drivers. For each driver, five mean curves from the different headings are shown, obtained from 10 trials per heading. Data for the blank condition were similar to that shown in Figure 5.

For both the constant feedback and blank conditions, the maximum steering angle reached during the first phase increased with increasing heading angle. This was true for all drivers, despite the varied strategies used to execute the task. Figure 6A and 6B display the maximum steering angle as a function of heading for the 6 drivers, for the constant feedback and blank conditions, respectively. These figures highlight the difference in steering amplitude across drivers, as well as the consistent increase in maximum steering angle with increased heading. Under constant visual feedback, the average increase in the maximum steering angle between the smallest and largest headings was 7.8° and 7.0° for the speeds of 20 and 25 m/s, respectively. For the blank condition, this average increase was 5.3° and 6.0° for 20 and 25 m/s, respectively. Figure 6C summarizes the dependence of maximum steering angle on heading across drivers. Given the large variation in steering amplitude across drivers, we normalized the individual driver data by their mean. We first calculated for each driver the difference between the maximum steering angle achieved for each heading and the mean of this angle across all headings. We then averaged these differences over the 6 drivers and plotted this average as a function of heading in Figure 6C. Data are shown for the 25 m/s speed condition; data for the 20 m/s condition were similar. A two-way analysis of variance (ANOVA)

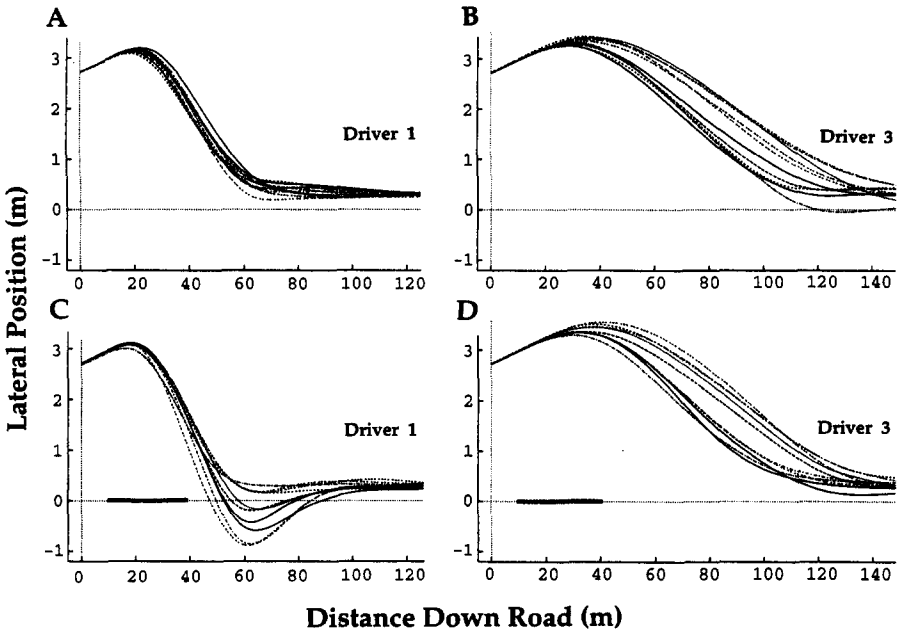

Figure 4. Position data from individual trials. The lateral position of the car as a function of distance down the road (both measurements in meters). Panels A and B show data for the constant feedback condition. Panels C and D show data for the blank condition. The blank screen was present roughly from 10 to 40 m down the road, as highlighted by a bold line on the horizontal axis. Panels A and C show data for Driver 1. Panels B and D show data for Driver 3.

combining data across heading and across the constant feedback and blank conditions shows a significant effect of heading on maximum steering angle: for 20 m/s, $F(4, 50) = 44.882$, $p = .0001$; for 25 m/s, $F(4, 50) = 97.412$, $p = .0001$. The data in Figure 6C suggest a possible interaction between the constant feedback or blank condition and heading. This effect was significant only for the 25 m/s speed condition, $F(4, 50) = 3.164$, $p = .0215$.

Comparing the data for the constant feedback and blank conditions, we noticed that some drivers reached a slightly larger maximum steering angle in the blank condition; however, overall, this effect was not significant. There was a small increase in the variability of steering activity in the blank condition. A two-way ANOVA revealed that the difference in the standard deviation of the maximum steering angle that was reached during the first phase between the constant feedback and blank conditions was significant only for the 25 m/s speed condition: On average, the standard deviation was 2.2° for the constant feedback condition and 2.85° for the blank condition, $F(1, 50) = 7.457$, $p = .0087$.

With regard to the duration of the maneuver, for some drivers the first zero-crossing of the steering angle profile occurred around the end of the blank period. For others, it occurred as much as 2 s later. There was no consistent effect of changes in heading on timing as measured by this zero-crossing. For some drivers, the variability of the zero-crossing time as measured by its standard deviation was slightly higher in the blank condition, but overall this effect was not significant.

To further assess differences in variability of performance between the constant feedback and blank conditions, we examined the standard deviations of the steering angle and lateral position of the car at the time that vision returned in the blank condition (2 s after the initial flash). These standard deviations were slightly higher in the blank condition (on average, the *SD* of steering angle increased by 0.4° in the blank condition relative to the constant feedback condition, and the *SD* of lateral position increased by 0.02 m). Two-way ANOVAs that combined the standard deviations of each of these two properties across headings and across the constant feedback and blank conditions indicated that this effect was not significant.

These results suggest that the heading of the car at the start of the maneuver, or some property that varies with heading, affects the amplitude of subsequent steering actions used to turn the car toward the midline. The temporal extent of the first phase of the maneuver appears not to be affected consistently by the initial heading. The first phase of the steering trajectory can be executed without visual feedback for 1.5 s without increasing the variability of its amplitude or temporal extent. The changes in heading used in this experiment are within a range that can be discriminated perceptually. Human observers achieve an accuracy of at least 1° of visual arc when translating with high speed and looking in their direction of heading (Crowell & Banks, 1993; van den Berg, 1992; Warren & Hannon, 1990). Riemersma (1981) measured drivers' ability to detect changes in heading and lateral position from computer displays consisting of road edges and a horizon. He concluded that drivers were sufficiently sensitive to small changes in heading and lateral position for these properties to underlie steering control during straight road driving.

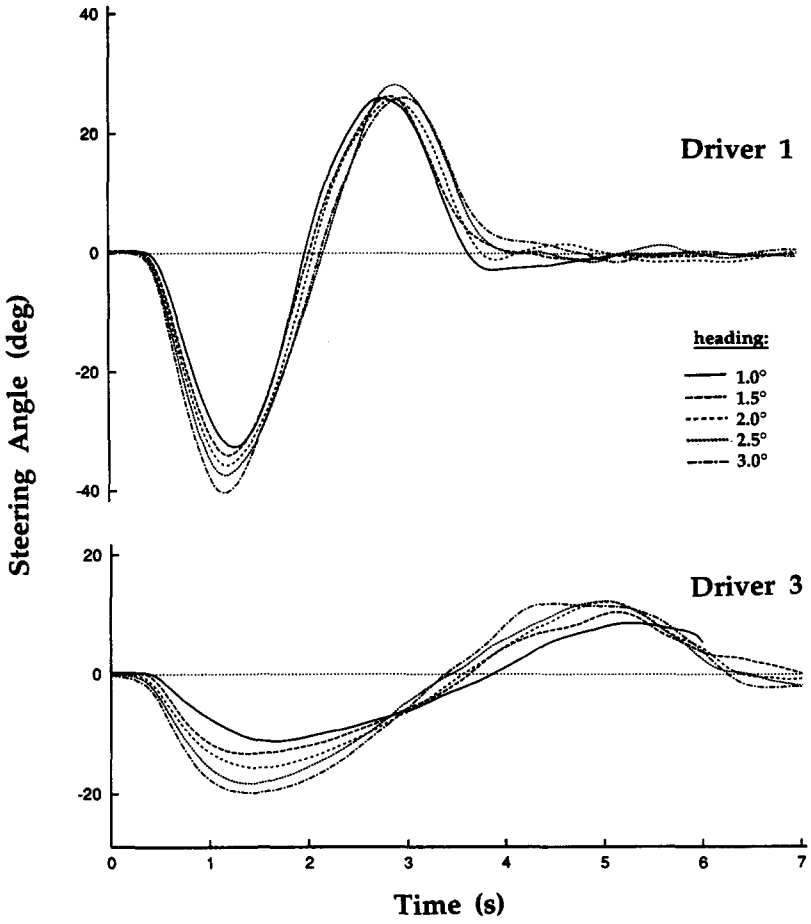

Figure 5. Mean steering angle data for different headings, with constant feedback. Data are shown for Drivers 1 and 3. Each of the five superimposed curves is an average of the 10 steering angle profiles obtained for individual trials, for the 25 m/s speed condition. The figure legend shows the heading corresponding to each curve.

Experiment 2: The Effect of Speed

Procedure. In this experiment, the heading and lateral position of the car at the start of the maneuver were held constant at 2.0° and 2.7 m, and speed was varied over five values: 17.5, 20.0, 22.5, 25.0, and 27.5 m/s. This experiment was conducted in two blocks of 50 trials. Each block contained 10 trials for each of the five speeds, presented in a random order. The constant visual feedback and blank conditions were presented in separate blocks. Prior to each test block of 50 trials, drivers performed 10 practice trials with 2 trials for each speed.

Results and discussion. The primary effect of a change in speed is an adjustment in the time course of the steering trajectory. Figure 7 shows mean steering angle data for 2 drivers, for each of the five speeds and for the constant visual feedback condition. The most apparent property of these curves is the change in timing with speed. All drivers performed the maneuver more quickly as speed increased, which is seen in the leftward shift of the first zero-crossing. This dependence of timing on speed occurred for both the constant feedback and blank conditions. Figure 8A and 8B show the zero-crossing time as a function of speed for individual drivers for the constant feedback and blank conditions, respectively. This figure highlights the difference in absolute timing across drivers and the consistent decrease in temporal extent with increasing speed. The average decrease in the zero-crossing time across speeds was 0.99 and 1.12 s for the constant feedback and blank conditions, respectively. Figure 8C summarizes this property of the data. Given the large variation in timing across drivers, we again normalized the data by their mean. For each driver, we first calculated the difference between the time of the zero-crossing for each speed and the mean of this time across all speeds. We then averaged these differences over the 6 drivers and plotted this average as a function of speed in Figure 8C. A two-way ANOVA showed a significant effect of speed on zero-crossing time, $F(4, 50) = 45.614, p = .0001$. Individual drivers showed an increase in the time of the zero-crossing in the blank condition, but overall this effect was not significant. The variability of timing, as measured by the standard deviation of the zero-crossing time, did not vary significantly between the constant feedback and blank conditions.

There was no effect of speed on the maximum steering angle achieved during the first phase. Individual drivers showed an increase in steering amplitude in the blank condition, but overall this effect was not significant. These data suggest that speed has

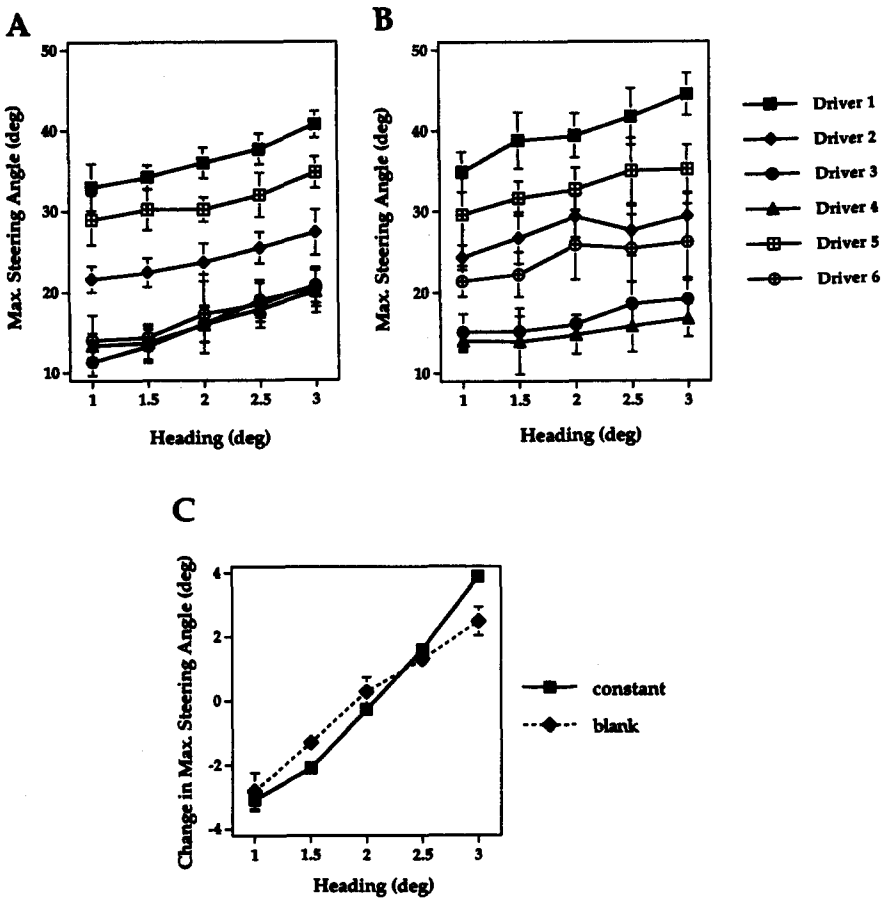

Figure 6. The effect of heading on maximum steering angle for individual drivers. Panels A and B: Data shown were obtained from the constant feedback and blank conditions, respectively, and were from the 25 m/s speed condition. For each driver, the maximum steering angle achieved during the first phase of the maneuver is plotted as a function of initial heading. Error bars indicate a single standard deviation. Panel C: Summary data for the effect of heading on maximum steering angle. Solid and dotted curves show data for the constant feedback and blank conditions, respectively, for the 25 m/s speed condition. Error bars show standard errors. Max. = maximum.

little effect on the amplitude of the initial steering actions. The lack of vestibular feedback could potentially reduce the influence of speed relative to natural driving conditions. Note that if lane corrections are made in a real car in such a way that steering amplitude remains constant, whereas timing is adjusted for different speeds, drivers would experience the same lateral acceleration at faster speeds, but jerk—the derivative of lateral acceleration—would increase.

With regard to the variability of steering performance, there was a small but significant increase in the standard deviation of the maximum steering angle between the constant feedback and blank conditions, as shown by a two-way ANOVA: On average, the standard deviation was 2.3° for the constant feedback condition and 3.0° for the blank condition, $F(1, 50) = 7.951$, $p = .0069$. We again examined the standard deviations of the steering angle and lateral position of the car in the two conditions at the time that visual feedback returned in the blank condition. These standard deviations were slightly higher in the blank condition (on average, the *SD* of steering angle increased from 3.65° to 5.12°, and the *SD* of lateral position increased from 0.21 to 0.24 m). In both cases, the effect did not reach a .05 significance level in a two-way ANOVA.

In the blank condition, 3 drivers completed all or most of the first phase of the steering maneuver during the blank period. Others did not complete this phase until 1–3 s after vision returned. For most drivers, changes in the timing of their steering with speed could be seen within the blank period. Drivers initially turned the steering wheel in a stereotyped way that reached a similar maximum angle for all speeds. The adjustment of timing is most apparent during the turn of the wheel from the left back to the 0° position. These observations suggest that speed, or some other property that varies with speed, affects the timing of subsequent steering actions to maneuver the car back to the midline. Again, the first phase of the steering trajectory can be executed without visual feedback for 1.5 s without significantly increasing the variability of its amplitude and temporal extent. Several studies have measured drivers' ability to estimate speed in real driving conditions (for review, see Evans, 1991) and report average errors

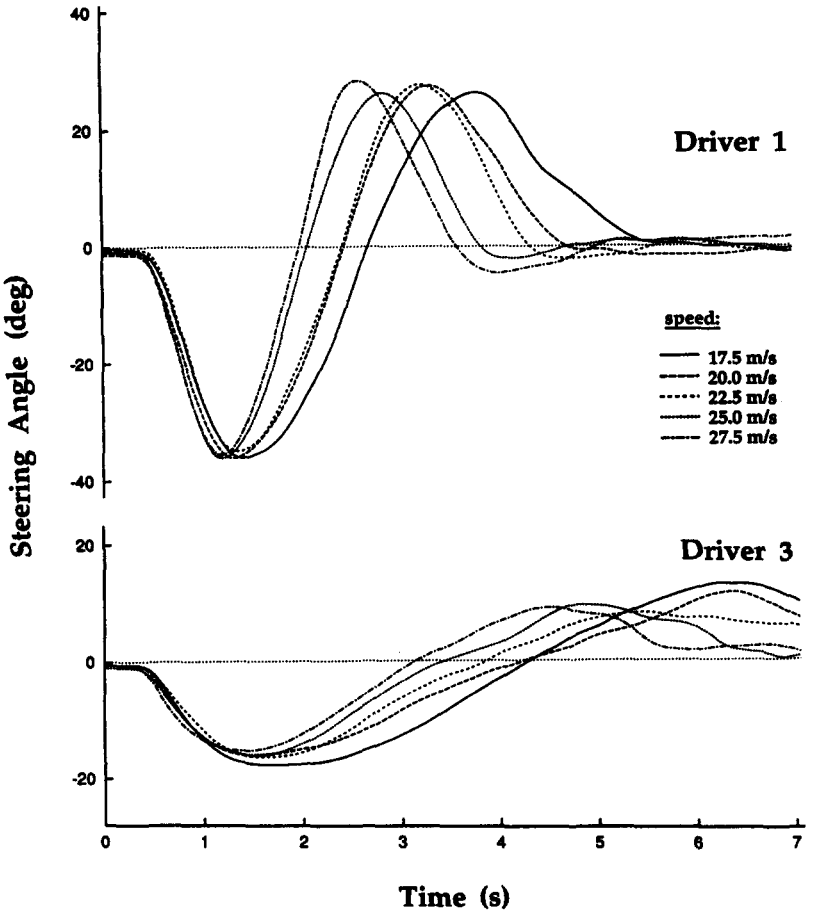

Figure 7. Mean steering angle data for different speeds, with constant feedback. Data are shown for Drivers 1 and 3. Each of the five superimposed curves is an average of the 10 steering angle profiles obtained for individual trials. The figure legend shows the speed corresponding to each curve.

of less than 2 m/s, suggesting that the speeds used in our experiments can be discriminated from one another.

Experiment 3: The Effect of Lateral Position

Procedure. In this experiment, the initial heading was held constant at 2.0° and speed was held constant at 20 m/s, but the time of the flash was varied so that the lateral position of the car at the start of the maneuver varied over five values: 1.38, 1.73, 2.08, 2.43, and 2.78 m to the right of the midline. This experiment was conducted in two blocks of 50 trials. Each block contained 10 trials for each of the five lateral positions, presented in a random order. The constant visual feedback and blank conditions were presented in separate blocks. Prior to each test block of 50 trials, drivers performed 10 practice trials, with 2 trials for each lateral position.

Results and discussion. There was no consistent effect of lateral position on the first phase of the steering action. Figure 9 shows mean steering angle data for 2 drivers, for the five lateral positions and the constant feedback condition. Data for the blank condition were similar to that of the constant feedback condition. Most drivers showed little variation in the first phase of the steering angle profile for different lateral positions. Figure 10A and 10B show the maximum steering angle and time of the first zero-crossing, respectively, as a function of lateral position. Data from the constant feedback condition are shown; data from the blank condition were similar to that of the constant feedback condition. A two-way ANOVA showed significant effects of lateral position on maximum steering angle, $F(4, 50) = 6.741$, $p = .0002$, and zero-crossing time, $F(4, 50) = 8.77$, $p = .0001$, but the size of these effects is very small. On average, the maximum steering angle increased by only 1.7°, and the zero-crossing time increased by only 0.18 s over the range of lateral positions tested.

There was no significant difference in the standard deviations of the maximum steering angle or zero-crossing time between the constant feedback and blank conditions. We also examined the standard deviations of the steering angle and lateral position of the car at the time that vision returned in the blank condition. These standard deviations were again slightly higher in the blank condition (on average, the *SD* of steering angle increased from 3.73° to 5.1°, and the *SD* of lateral position increased from 0.16 to 0.17 m) but did not reach the .05 level of significance in a two-way ANOVA.

We conclude that lateral position at the start of the maneuver has little effect on the first phase of the steering trajectory. For the

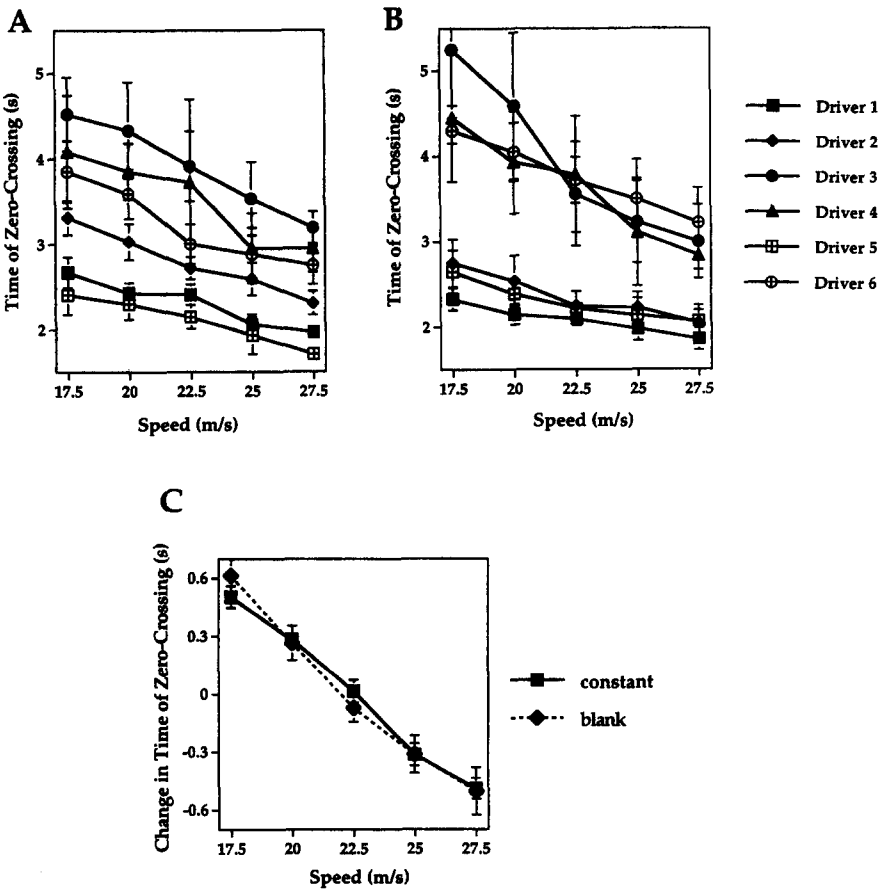

Figure 8. The effect of speed on zero-crossing time for individual drivers. Panels A and B: Data for the constant feedback and blank conditions, respectively. For each driver, the zero-crossing time is plotted as a function of speed. Error bars indicate a single standard deviation. Panel C: Summary data for the effect of speed on the timing of the zero-crossing. The solid and dashed curves show data for the constant feedback and blank conditions, respectively. Error bars show standard errors.

driver to complete the maneuver successfully, the second phase of the steering profile must vary as lateral position is increased because the car must cover a larger distance to return to the center line. Most drivers appear to start the maneuver with a highly consistent turn of the car to point toward the center line that does not depend on lateral position. The different initial starting positions are then accommodated through adjustments of the rotation of the wheel during realignment of the car with the midline.

Experiment 4: The Effect of Varying the Duration of Visual Occlusion

The previous experiments held the duration of the blank period constant at 1.5 s. Drivers may have anticipated this fixed blank period and used a steering strategy to accommodate this occlusion time that does not reflect their general behavior during arbitrary times of reduced visual input. In addition, our data show that drivers can steer through a 1.5-s blank period without substantially increasing the variability of their performance and without disrupting their ability to complete the task upon the return of visual feedback. In this final experiment, we varied the duration of the blank period between trials and extended its length. Note that we could also have manipulated the time of onset of the blank period, but this would have reduced control over the visual conditions present at the start of visual occlusion if the onset occurred after the driver had begun to turn the steering wheel and rotate the car.

Procedure. This experiment was conducted in four blocks of 90 trials. In three of the blocks, a blank period was present on every trial, which began 0.5 s after the flash and lasted for 1, 2, or 4 s. In one of these three blocks, we also varied the initial heading (speed and initial lateral position were held constant at 25 m/s and 2.7 m, and heading was 1.0°, 2.0°, or 3.0°). In the second block, we varied speed (the heading and lateral position at the time of the flash were held constant at 2.0° and 2.7 m, and speed was 17.5, 22.5, or 27.5 m/s), and the third block varied the lateral position at the start of the maneuver (heading and speed were held constant at 2.0° and 25 m/s, and lateral position was 1.38, 2.08, or 2.78 m). In the fourth block, all trials were conducted with constant visual feedback, and nine conditions were presented that included each set of three conditions that varied heading, speed, and lateral position used in the three blocks described above. Each block contained 10 trials for each of nine conditions, presented in a random order. Prior to each block, drivers performed 9 practice trials that contained 1 trial for each condition. One of the drivers who participated in the previous experiments (Driver 4) was not available

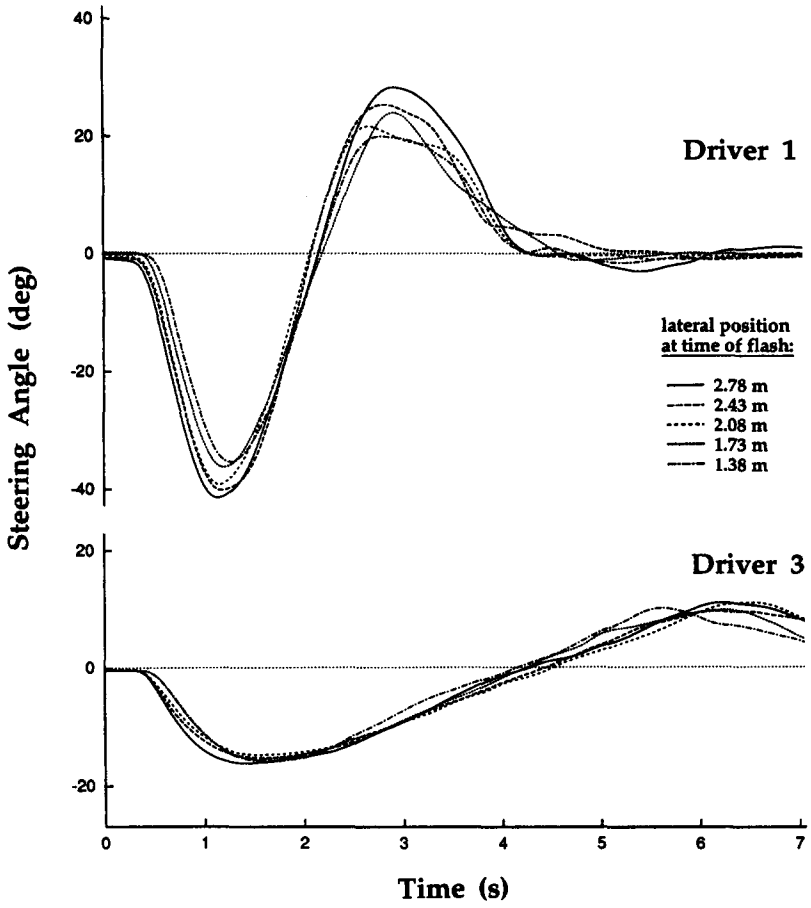

Figure 9. Mean steering angle data for different lateral positions, with constant feedback. Data are shown for Drivers 1 and 3. Each of the five superimposed curves is an average of the 10 steering angle profiles obtained for individual trials. The figure legend shows the lateral position corresponding to each curve.

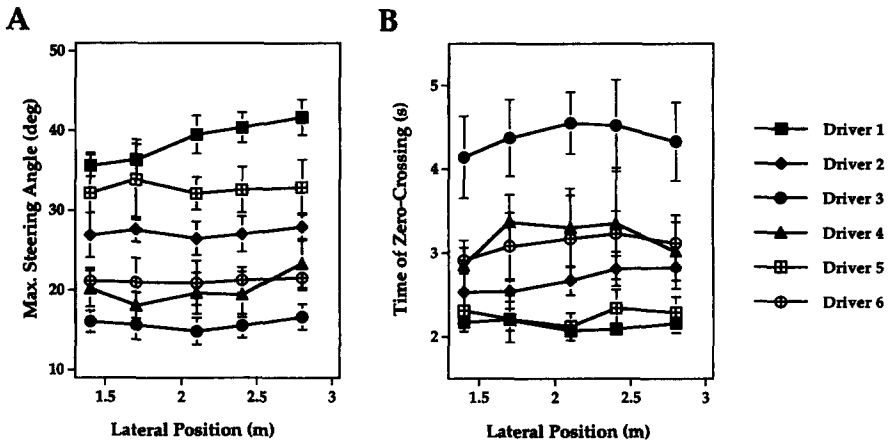

Figure 10. The effect of lateral position on maximum steering angle and zero-crossing time for individual drivers. For each driver, Panel A plots the maximum steering angle as a function of lateral position, and Panel B plots the zero-crossing time as a function of lateral position. Only data for the constant feedback condition are shown. Error bars indicate a single standard deviation. Max. = maximum.

for this final experiment and was replaced with another driver who was naive about the purpose of the experiments.

Results and discussion. The data from this experiment reinforced the observations made earlier. The maximum steering angle reached during the first phase of the steering action consistently increased with increasing heading, and the temporal extent—as measured by the time of the first zero-crossing—decreased with increasing speed. Even when variations in heading, speed, and lateral position were combined in the block of constant feedback trials, these main effects emerged for all drivers. Similar to previous experiments, there was a small increase in the variability of steering performance in the blank conditions, as measured by the standard deviations of the maximum steering angle and zero-crossing time. For trials in which a blank period was present, steering behavior during the first 1–2 s after the flash was similar to that observed previously when the blank period was fixed at 1.5 s. We focus our analysis here on what happens to steering performance after the first 2 s, when the blank period extends for 4 s.

Two of the 6 drivers (Drivers 1 and 2) maintained a sinusoidal steering action through the 4-s occlusion period and continued to show consistency of the amplitude and time course of their steering in response to the initial visual conditions. Data from Driver 1 are shown in Figures 11 and 12. Figure 11A shows steering profiles for 10 individual trials for one condition (initial heading 3.0°, speed 25 m/s, and lateral position 2.7 m). Variability of the steering angle was similar throughout the 4 s. Vision returned at 4.5 s and was followed by large steering corrections that start around 5 s. Figure 12 shows the mean steering angle data for this driver, obtained for the different heading, speed, and lateral position conditions. As heading was increased, steering amplitude increased throughout the 4-s blank period with little adjustment of its temporal extent (Figure 12A). Figure 12B shows a continued modulation of the temporal extent of the steering profile with little adjustment in amplitude. In Experiment 3, Driver 1 showed an increase in amplitude and no adjustment of timing, with increasing lateral position. This behavior continued through the 4-s blank period, as shown in Figure 12C. Although Driver 1 maintained a consistent steering action for an extended time, the performance of the task was severely degraded. This is illustrated in Figure 11B, which shows the lateral position of the car as a function of time for the 10 trials whose steering profiles appear in Figure 11A. Without visual feedback to make steering corrections, drivers end up making large lateral-position errors. Most drivers were unable to maintain a consistent steering pattern beyond the first 2 s of occlusion and used steering strategies that may reflect large uncertainty about the state of the car. These include the execution of very slow steering changes, the use of long holds of the steering wheel around one position with small adjustments superimposed, and very high variability in steering throughout the blank period.

In general, beyond about 1.5 s of occlusion, the driver's steering action is no longer adequate to complete the task successfully. This is highlighted in Figure 13. Figure 13A shows the standard deviation of the steering angle at the time of return of visual input for the 1, 2, and 4-s blank conditions (dashed curve) and at these same times (1.5, 2.5, and 4.5 s) in the continuous feedback trials (solid curve). Data were collapsed over all drivers and all heading, speed, and lateral-position conditions. The variability in steering angle was higher for the blank conditions than for the constant feedback

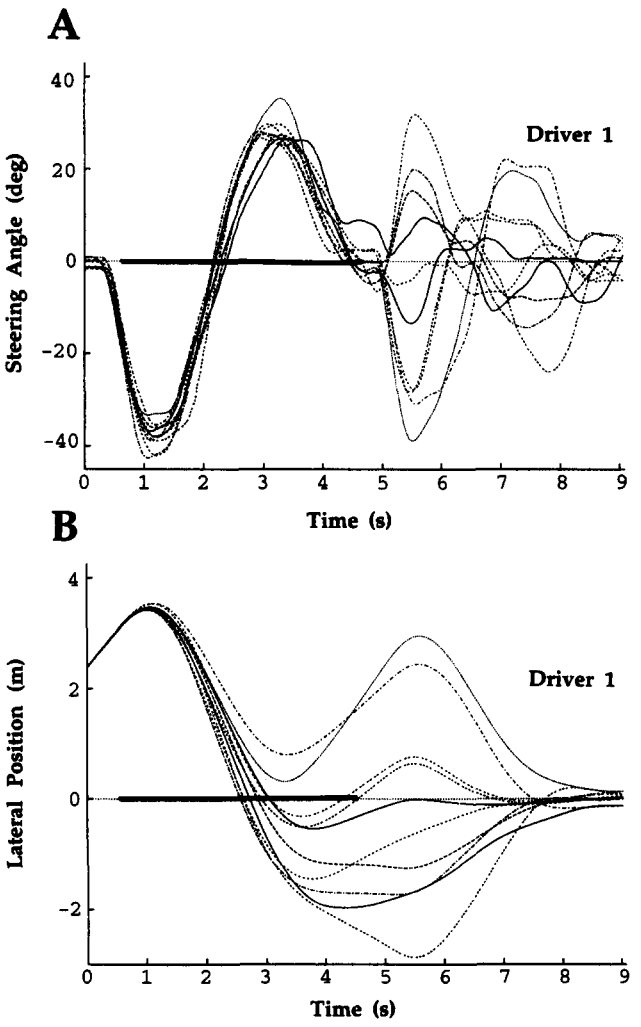

Figure 11. Individual driver performance for the 4-s blank period. A: Steering profiles for the 10 individual trials obtained for Driver 1 for the following initial conditions: heading 3.0°, speed 25 m/s, and lateral position 2.7 m. B: The spatial paths of the car, shown as lateral position as a function of time, for the 10 trials whose steering profiles appear in Panel A. The blank period is highlighted on the horizontal axis of each graph by a bold line.

conditions. In both cases, the variability increased up to 2 s and then leveled off. The variability in lateral position increased dramatically in the extended blank conditions. Figure 13B shows the standard deviation of lateral position at the time of return of visual input for the 1, 2, and 4-s blank conditions (dashed curve) and at these same times in the continuous feedback trials (solid curve). For the constant feedback condition, the variability of lateral position remained roughly constant, but this variability increased substantially for the 2- and 4-s blank conditions. For the blank condition, the increase in the standard deviation of steering angle between 1.5 and 2.5 s reflects the effect of error correction. The large variability in lateral position after a 4-s occlusion period is largely due to the fact that even small heading deviations toward the completion of the task eventually result in large lateral deviations if the driver does not have visual input to correct for the

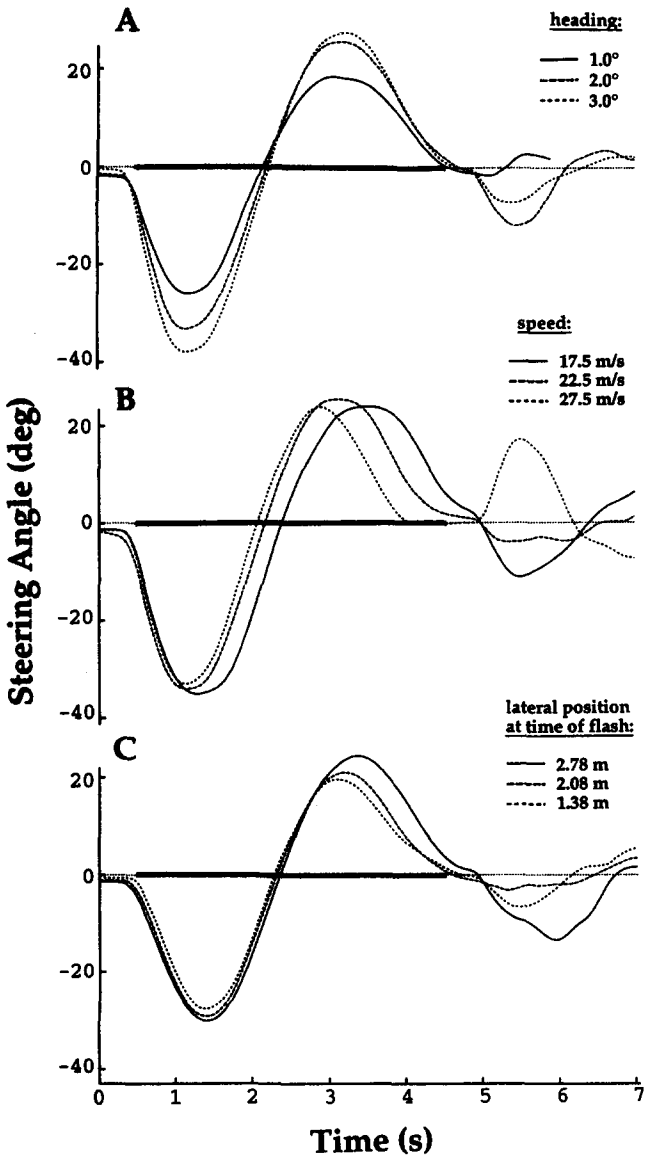

Figure 12. Individual driver performance for the 4-s blank period: mean steering angle data (averaged over 10 trials) for different initial headings (Panel A), speeds (Panel B), and lateral positions (Panel C) for Driver 1. The blank period is highlighted on the horizontal axis of each graph by a bold line.

heading errors. We conclude that for the task used in our experiments, drivers can maintain a viable steering action only for a short time of about 1.5 s.

Summary of Main Experimental Findings

We measured drivers' performance of a lane correction task in which the visual conditions at the start of the maneuver and the duration of a brief occlusion period during execution were systematically varied. Below are the main findings that we want to capture with the behavior of our models of steering control.

1. For all drivers, the amplitude of the initial steering action increased with the initial heading (see Figure 6). There was no consistent change in the timing of steering actions with heading.

2. For all drivers, the time over which the steering maneuver was completed decreased as speed increased (Figure 8). There was no change in steering amplitude with speed.

3. There was little or no change in the amplitude or timing of initial steering actions with changes in lateral position at the start of the maneuver (Figure 10).

4. In absolute terms, the amplitude and timing of steering actions varied considerably across drivers. At one extreme were drivers with high amplitude and rapid steering changes, and at the other extreme were drivers with low amplitude and slow steering changes. The relative effects of the experimental conditions were similar across drivers.

5. The above steering behaviors were also observed during a period of visual occlusion that began 0.5 s after the driver was signaled to start the maneuver (Figures 6C and 8C, dashed curves).

6. Drivers could tolerate 1.5 or 2 s of visual occlusion without severe degradation in task performance (Figure 13), as measured by the standard deviation in the lateral position and steering angle immediately following the occlusion period. With a 4-s blank period, 2 drivers maintained a consistent steering pattern, whereas the other 4 drivers exhibited substantial variability in their steering after the first 2 s of blank time. All drivers showed severe degradation in task performance with 4 s of occlusion.

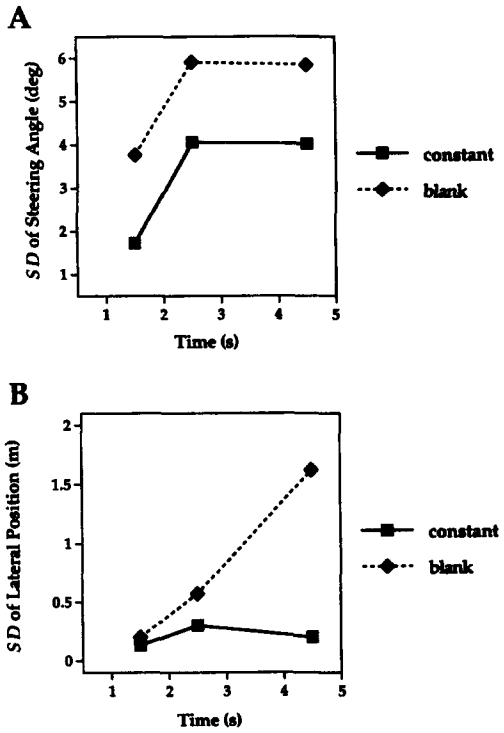

Figure 13. Variability of driver performance during extended blank periods. A: Standard deviation of the steering angle at the time of return of visual input for the 1-, 2- and 4-s blank conditions and for these same times in the constant feedback trials. B: Standard deviation of the lateral position of the car at the time of return of visual input for the 1-, 2- and 4-s blank conditions and for these same times in the constant feedback trials.

Although our experiments were conducted in the virtual world of a driving simulator, we believe that the results reflect elements of real driving behavior. This is supported by the consistent and systematic way that individual drivers responded to the visual conditions presented in the display, the consistency of the trends seen across all drivers, and the ability of all drivers to execute appropriate steering changes during short periods of visual occlusion with little increase in variability. The latter ability presumably draws on participants' prior driving experience in similar, real contexts.

Models of Steering Control

This section relates the experimental results to two fundamentally different models of steering control. The first model uses PD control (Dorf & Bishop, 1995) to regulate the state of perceptual variables that are relevant to the lane correction task. In the second model, the driver continually pursues a virtual target in the environment while performing a lane correction. This modeling effort accomplishes several goals. Most importantly, it allows us to summarize the experimental results in a single theoretical framework. We formulate each model in a way that yields behavior that is affected by the initial conditions of a lane correction, similar to that of human drivers. Through the PD control model, we address to what extent the regulation of perceptual variables is adequate to explain driver performance and whether prediction and preview of the future state of the vehicle and environment are necessary. We find that drivers' steering actions during lane corrections are described well by a PD control model in which steering changes are made in direct response to the current state of a small set of perceptual variables. The target model embodies a very different approach to steering control, one in which the car is effectively pulled through the environment by a virtual target that is defined by the driver. This model also produces steering behavior that closely matches the details of human steering data. We believe that the target model has greater explanatory power and can be extended more easily to other steering tasks.

With both models, we examine whether the large intersubject variability can be accounted for by simply changing model coefficients. Finally, we examine how these models can continue control during visual occlusion. We explore whether control during brief occlusions can be based on a continuous extrapolation of the model input that is normally derived from visual feedback. This extrapolation requires the driver to have an internal model of how steering actions affect the state of the car. We show that with reasonable assumptions about the error sources that arise, both models can use extrapolation to control steering during occlusion, with a pattern of degradation in performance that is similar to that of human drivers.

Steering Control Model 1: Regulation of Perceptual Variables

We first consider whether human steering performance during lane corrections can be explained by a model in which steering actions are directly coupled to the state of one or more perceptual variables. In this approach, appropriate perceptual variables are chosen to assess task performance, and steering is continually adjusted to drive these variables to a desired value that is typically zero. For lane corrections, the most plausible perceptual variables include lateral position and heading relative to the lane boundaries and temporal derivatives of these variables. Given the straight road and viewing geometry used in our displays, we note that lateral position is related directly to *splay angle,* which is the angle between the projected lane boundary and the vertical direction (Beall & Loomis, 1997; Riemersma, 1981). Splay angle and its temporal derivative could also serve as perceptual variables to be regulated. At the successful completion of a lane correction, all of the above variables are zero.

Many standard control algorithms can be applied to steering control during lane keeping. Each defines a performance index that embodies criteria that are specific to the task and generates a control signal that optimizes this performance index (Dorf & Bishop, 1995). The performance index is typically a quadratic cost function that can include terms that depend on the individual perceptual variables and their derivatives (in the case of PD controllers) as well as interactions between variables (in the case of optimal control; Levison & Cramer, 1995; Lewis and Syrmos, 1995; Sheridan & Ferrell, 1981). The performance index can also depend on the control activity itself. For example, the addition of a term that depends on the rate of change of steering angle penalizes rapid wheel rotations that could result in large changes in lateral acceleration. A gain factor is associated with each term of the cost function that reflects the relative contribution of each perceptual variable to steering changes at each moment. The control algorithm can be a pure regulator, in which errors in the current state of the perceptual variables are used to make immediate steering corrections. Alternatively, a predictive capability can be added so that the control algorithm minimizes the deviation between the predicted and desired state of the perceptual variables at a future time or over a time window up to a time horizon.

Formulation of the PD control model. Exploratory analysis of a variety of model formulations suggested that drivers' steering actions are captured well by a PD control model composed of two parts. The first computes a desired steering angle at each moment from the vehicle's current lateral position and its first and second temporal derivatives. The second computes the final steering angle to be applied after imposing driver limitations on the maximum rate at which the steering wheel can be rotated and how quickly this rotation rate can be changed. We first derive the equations used to compute the desired steering angle and then describe how driver limitations are incorporated and how the human data were used to obtain a final model.

As stated above, the most plausible perceptual variables to be controlled during a lane correction are lateral position, heading, and their temporal derivatives. We first express the desired yaw rate at each moment, Y_d (the rate of rotation of the car), as a weighted sum of these four perceptual variables:

$$Y_d = \alpha\delta_n + \lambda\psi_n + \beta\delta'_n + \gamma\psi'_n, \quad (1)$$

where δ_n is the current lateral deviation from the midline, ψ_n is the vehicle's current heading with respect to the road, and δ'_n and ψ'_n are the temporal derivatives of these variables. Given the small range of heading that is covered during a lane correction, ψ_n and ψ'_n are related to lateral position and its derivatives through the car's speed, v:

$$\psi_n \approx \delta'_n/v \quad \text{and} \quad \psi'_n \approx \delta''_n/v,$$

where δ_n'' is the second temporal derivative of δ_n. Substituting these two expressions into Equation 1 yields

$$Y_d = \alpha\delta_n + (\lambda + \beta v)(\delta_n'/v) + \gamma(\delta_n''/v). \quad (2)$$

The weight associated with the δ_n'/v term in Equation 2 is a linear function of speed, whereas the weights on the other two terms do not vary with speed. We found that a closer match between the model results and human data can be obtained if the weights α and γ also vary linearly with speed. This leads to the following expression for Y_d (the coefficient λ in Equation 2 is replaced with β_0):

$$Y_d = (\alpha_0 + \alpha_1 v)\delta_n + (\beta_0 + \beta_1 v)(\delta_n'/v) + (\gamma_0 + \gamma_1 v)(\delta_n''/v). \quad (3)$$

Given the mapping between yaw rate and steering angle for a particular vehicle, which is assumed to be known by the driver, we can compute a desired steering angle, θ_d, from Y_d (see Appendix A for details). We refer to this mapping as the *car model.* The expression for Y_d in Equation 3 leads to a final PD control model with the same complexity, in terms of the number of coefficients, as the target-based model that we develop later. This part of the model suggests that drivers assign costs to the perceptual variables that are proportional to the controller coefficients. Formulations that use fewer terms to describe Y_d result in steering behavior that does not match human steering data as well. More complex formulations—for example, those with additional terms that capture interactions between input variables—do not improve the fit between the model and human data.

The desired steering angle, θ_d, cannot be reached by the driver instantaneously, owing to limitations of the motor system. A third-order linear filter was used to model driver limitations. This filter, described in Appendix A, is characterized by three coefficients: ζ, which is a damping factor; p, which affects the rate of response of the filter and the extent of overshoot of a desired output; and ω_n, which is the natural frequency at which the filter would oscillate if it were undamped. We found a third-order filter to be the lowest order linear filter capable of characterizing drivers' smooth steering movement characteristics. In addition to this filter, a pure response delay was imposed at the start of the maneuver. This reflects the time needed for the driver to assess the visual conditions and initiate a motor response. As suggested by the data, this delay was set at 0.4 s. We refer to the combination of this third-order filter and response delay as the *driver model.*

Given the initial conditions of a lane correction, Equation 3—together with the car model and driver model—can be used to generate an entire steering profile by continually recomputing a new vehicle state based on the newly computed steering angle. Model coefficients can be identified that result in the best match between the extended steering and lateral-position profiles generated by the model and those observed for human drivers. Details of this derivation are given in Appendix A.

Simulations with the PD control model: Results and analysis. The performance of this PD control model suggests that the simple characterization of steering changes as a direct response to a set of input variables results in steering behavior that is similar to that of human drivers. The computed steering profiles show the same dependencies of amplitude and timing on the visual conditions at the start of the lane correction. Figures 14 and 15 show a comparison between the results of the model and the data for Drivers 1 and 3, respectively. The computed model coefficients are given in the legends. We separately identified model coefficients for Drivers 1 and 3 using the mean steering and lateral-position profiles obtained from 15 initial conditions. Our development of both models used data from Drivers 1 and 3 because these two drivers exhibited the range of behavior observed across all 6 drivers (the extremes of amplitude and timing) and were highly consistent across trials. For reasons described in Appendix A, two sets of coefficients were identified for each driver. One set used data from Experiments 1 and 2, in which the initial heading and speed were varied, and the second set used data from Experiment 3, in which the lateral position at the start of the lane correction was varied. The top row of Figures 14 and 15 shows graphs of lateral position as a function of time, whereas the bottom row of each figure shows the steering angle profiles. Solid curves correspond to human data and dotted curves are model output. The left, middle, and right columns show results for different initial headings, speeds, and lateral positions, respectively. In each case, results for three values of heading, speed, and lateral position are shown. Note that the steering angle and time scales differ between Figures 14 and 15.

The PD control model produces position and steering profiles that closely follow the shape of human profiles and exhibit the main trends seen in the data. For both drivers, the amplitude of the steering profiles computed by the model increases with the initial heading, with no change in the timing of the actions. The temporal extent of the steering action decreases with increasing speed. For Driver 1, the amplitude of the first peak of the computed steering profiles does not change with speed, whereas for Driver 3, there is a slight decrease in this amplitude with increasing speed. Both of these relationships are also seen in the experimental data. When the initial lateral position is varied, the steering profiles generated by the model exhibit an increase in amplitude of the first peak with increasing lateral position. The human data show a small increase in amplitude, especially in the data from Driver 1, but the range of amplitudes obtained by the model is somewhat larger. Similar to the data, there is little variation in timing with changes in lateral position.

In the model results, the final return of the steering wheel to 0° at the end of the lane correction, when the car is realigned with the midline, occurs more slowly than observed in the human data. The model also produces slow oscillations of lateral position and steering angle after completion of the task. Both behaviors occur because the PD controller is essentially a linear digital filter that is second order in lateral position, combined with a third-order driver model. Like any such filter, the PD controller does not incorporate a notion of task completion (the target-based model differs in this respect). Second-order filters are defined by a natural frequency at which they oscillate and a damping factor that determines how quickly oscillations are damped out. If damping is large, then oscillations do not occur and the maximum possible rate of change in steering angle decreases (Ogata, 1990). The model coefficients identified from the human data strike a compromise, with a moderately fast response and small oscillations. Identification of the coefficients used data that extended 0.5 s beyond the time of completion of the lane correction. If more data are included in the analysis, the amplitude of the later oscillations is reduced, but the overall fit of the model to the data obtained during the first few seconds of the maneuver is degraded. Similarly, using less data yields a slightly better fit to the second phase of the steering

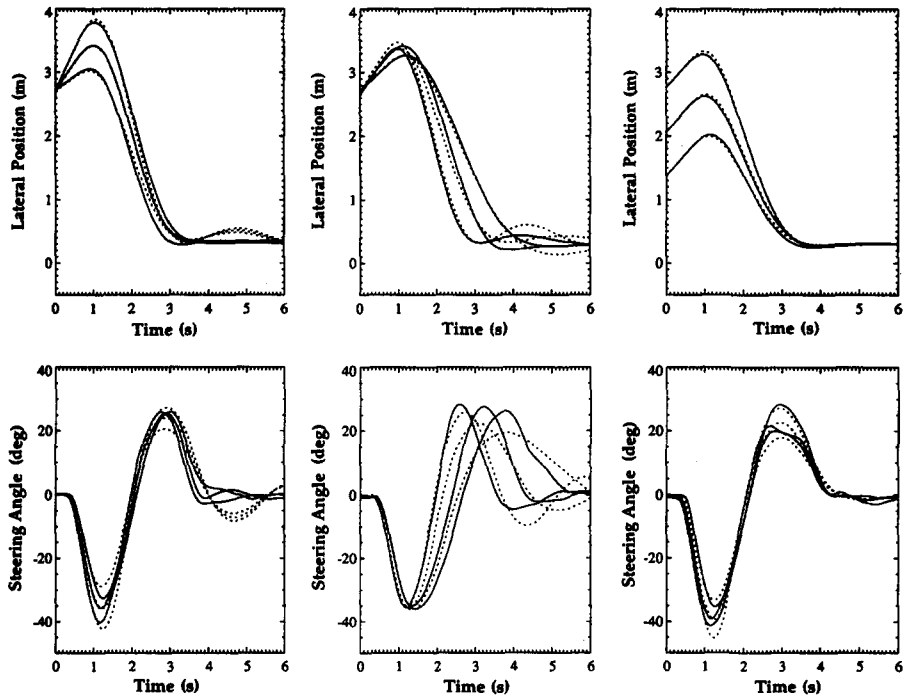

Figure 14. Comparison of the results of the proportional-derivative control model with steering data for Driver 1. Top row: Lateral position as a function of time. Bottom row: Steering angle profiles. Solid curves show human data from individual trials, and dotted curves show model output. Results are shown for three of the initial headings (1°, 2° and 3°; left column), speeds (17.5, 22.5, and 27.5 m/s; middle column), and lateral positions (1.38, 2.08, and 2.78 m; right column) used in Experiments 1–3. Computed model coefficients using data from Experiments 1 and 2 were $\omega_n = 7.710$, $\zeta = 0.896$, $p = 2.695$, $\alpha_0 = 0.002$, $\alpha_1 = 0.002$, $\beta_0 = -0.918$, $\beta_1 = 0.122$, $\gamma_0 = 1.342$, and $\gamma_1 = 0.064$. Model coefficients using data from Experiment 3 were $\omega_n = 6.332$, $\zeta = 1.574$, $p = 4.241$, $\alpha_0 = 0.022$, $\alpha_1 = 0.003$, $\beta_0 = -1.398$, $\beta_1 = 0.201$, $\gamma_0 = 1.743$, and $\gamma_1 = 0.645$.

trajectories, but the subsequent oscillations increase. Later, we discuss that these trade-offs do not arise for the target model.

It is difficult to provide simple, intuitive explanations for some of the behavior of the PD controller because of the complex interactions between steering actions and the input variables. Given the direct dependence of the steering change at each moment on lateral position (δ_n) and heading (δ_n'/v) in Equation 3, one would expect an increase in steering amplitude with increases in initial heading and lateral position. The explanation for the dependence of timing on speed is more complex. As speed increases, δ_n' increases, and once steering is initiated, δ_n'' also increases. Both effects result in a larger desired steering angle. The rate at which this larger value is approached is constrained by driver limitations. Little difference is seen in timing during the initial change of steering angle to its maximum value during the first phase because the initial rate of steering change is maximal for all speeds (reflecting driver limitations). After the car is turned to head toward the midline, the derivative in lateral position is again larger for higher speeds but has an opposite sign, which draws the steering angle faster toward a positive value. The steering rate during this part of the steering maneuver is below the maximum possible rate so a steeper slope in the steering profile results, causing it to reach the 0° position earlier.

Differences in behavior across drivers are captured well through changes in model coefficients. The higher amplitude, faster steering actions of Driver 1 are reflected primarily in larger weights associated with the three terms of Equation 3 that determine the desired yaw rate at each moment. The weights on the first two terms that depend on lateral position and its derivative, $\alpha_0 + \alpha_1 v$ and $\beta_0 + \beta_1 v$, are consistently larger for Driver 1 relative to those for Driver 3. Compared with Driver 3, Driver 1 makes larger steering adjustments in response to the same conditions, compressing the steering action over a shorter time. The weight on the third term of Equation 3 that depends on the second derivative of lateral position, $\gamma_0 + \gamma_1 v$, is positive for Driver 1 and negative for Driver 3. This suggests that the steering actions of Driver 3 are made to counteract large lateral accelerations more directly. For Driver 1, the driver model coefficients yield a temporal filter that effectively slows down their response to the visual input. For Driver 3, the driver model has relatively little affect on the overall response rate.

Steering control during visual occlusion. To continue control during visual occlusion, the PD controller must have an explicit model of how the input variables will change over time, given the current state of the vehicle and environment and particular control input. This internal model can be used to generate a predicted time sequence of perceptual input that can be used to update the control signal. In particular, given an internal model of how the current speed and steering angle affect the change in lateral position of the car over time, it is possible to predict changes in lateral position

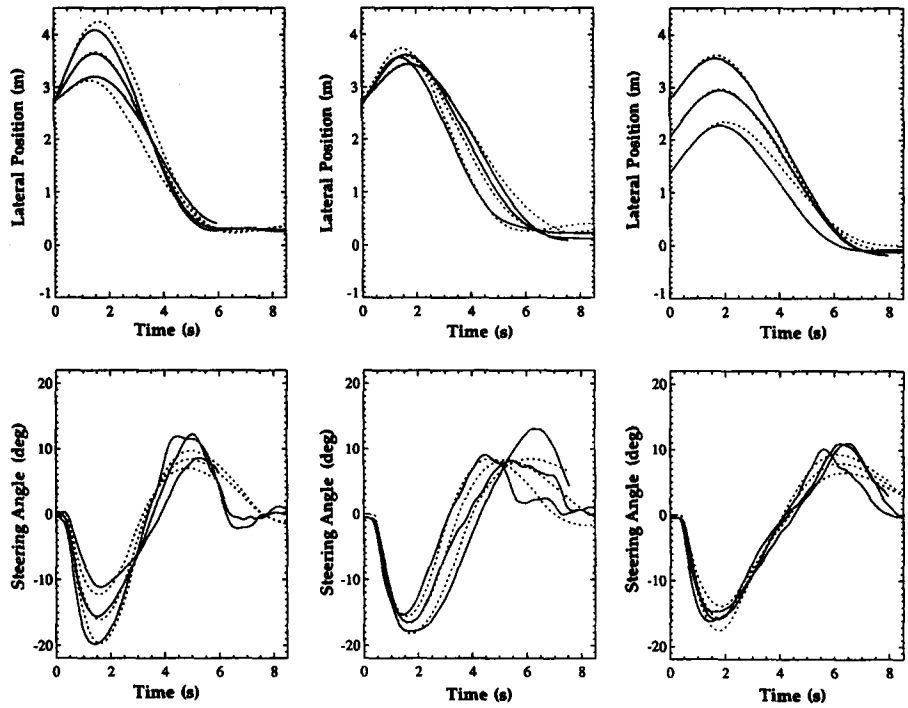

Figure 15. Comparison of the results of the proportional-derivative control model with steering data for Driver 3. Top row: Lateral position as a function of time. Bottom row: Steering angle profiles. Solid curves show human data from individual trials, and dotted curves show model output. Results are shown for three of the initial headings (1°, 2°, and 3°; left column), speeds (17.5, 22.5, and 27.5 m/s; middle column), and lateral positions (1.38, 2.08, and 2.78 m; right column) used in Experiments 1–3. Computed model coefficients using data from Experiments 1 and 2 were $\omega_n = 7.884$, $\zeta = 2.705$, $p = 22.036$, $\alpha_0 = 0.008$, $\alpha_1 = 0.0002$, $\beta_0 = 0.021$, $\beta_1 = 0.037$, $\gamma_0 = 1.565$, and $\gamma_1 = -0.106$. Model coefficients using data from Experiment 3 were $\omega_n = 6.124$, $\zeta = 8.908$, $p = 21.838$, $\alpha_0 = 0.338$, $\alpha_1 = -0.0137$, $\beta_0 = -0.602$, $\beta_1 = 0.194$, $\gamma_0 = -0.482$, and $\gamma_1 = 3.959$.

and its derivatives that should result from steering changes made over a short occlusion period. An extrapolation strategy of this sort would circumvent the need to plan and represent internally an extended steering trajectory to be executed during occlusion. This strategy has the advantage of being able to cope with occlusions that occur at any time and that have arbitrary duration.

We implemented this extrapolation strategy and examined the performance of the resulting model during brief occlusions. To conduct a rigorous test of this approach, we added noise to the following quantities: the initial heading, lateral position, and speed at the start of the lane correction; the six coefficients in Equation 3; the coefficients in the car and driver models; and the final steering angle that is executed at each moment. For the initial conditions and all model coefficients, 5% Gaussian-distributed noise was added. For the steering execution noise, we added a band-limited error signal to the computed steering profile. (During occlusion, the error signal had a bandwidth of 0.16 Hz and root-mean square amplitude of 0.03, and when visual input was available, the bandwidth was increased to 0.5 Hz, reflecting the expectation that drivers respond more quickly to execution errors when visual feedback is available.) The noise coefficients were chosen in part to yield similar performance to that of human drivers. Figure 16 shows the results obtained from the model, using the extrapolation of perceptual variables to continue control during occlusion, together with the above noise sources. Lateral position and steering profiles are shown in Figure 16A and 16B, respectively. The thick curve shows the result obtained when visual input is available throughout the maneuver and no noise is added. The thin curves show the results of 15 trials that contained a 4-s occlusion (shown highlighted on the horizontal axis). Over this long occlusion period, the resulting lateral-position error and the amplitude of the subsequent steering corrections that occur when vision returns are similar to those observed for Driver 1 (see Figure 11A and 11B). Further simulations showed that for shorter occlusions, this model also produces behavior comparable to that of Driver 1. This analysis suggests that a mechanism for extrapolating the state of the perceptual variables may be sufficient to maintain adequate steering control for short periods of time. Over longer occlusions, errors in the perceptual variables, internal models, and execution of steering actions will result in large performance errors, similar to those observed for human drivers.

Summary of the PD control model. The performance of the PD control model indicates the extent to which the simple regulation of relevant perceptual variables can account for human steering behavior. The shape of drivers' steering trajectories is captured well by this model, and the same dependencies of steering amplitude and timing on the initial visual conditions are seen in the results. The detailed shape of the steering profiles following the second peak, during the realignment of the car with the midline, is

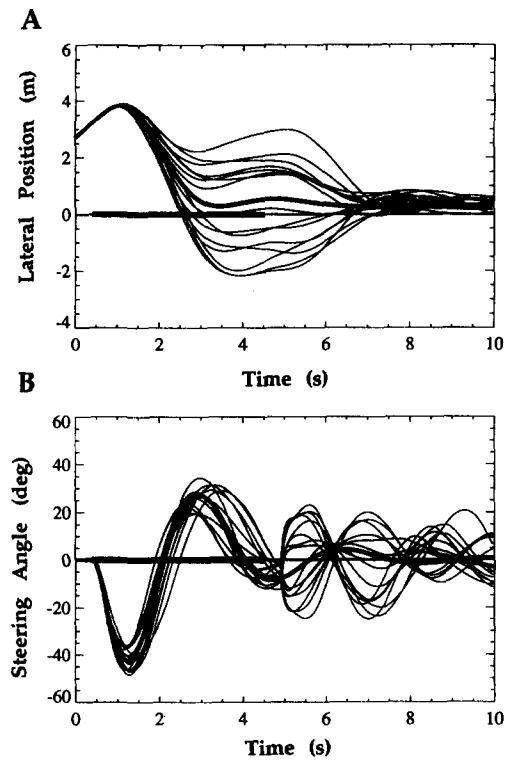

Figure 16. The results of the proportional-derivative control model under occlusion. Lateral position profiles (Panel A) and steering angle profiles (Panel B), obtained with added noise sources and extrapolation of the perceptual variables during occlusion. Thick line shows the results obtained under visual feedback with no noise, and thin lines show the results of 15 trials obtained with a 4-s occlusion period. The occlusion period is highlighted on horizontal axes of graphs by a bold line.

not reproduced well by the PD control model. The addition of a predictive or anticipatory component to the model might improve the fit between model and human performance. Some predictive capability was added to the model to continue control during brief visual occlusions. A mechanism based on the continuous extrapolation of the control input during occlusion may be sufficient to yield performance similar to that of human drivers.

To extend the PD control model to other steering tasks, it is necessary to define appropriate perceptual variables to assess task performance that can be regulated to a desired value. For lane changes, the variables could include lateral position and heading relative to a virtual center of the adjacent lane. For curve negotiation, one could regulate lateral position relative to a desired spatial path to follow through the curve. Defining appropriate perceptual variables for a range of steering tasks is challenging. For steering maneuvers that require a complex spatial path, it may be difficult for drivers to perceive their state relative to an arbitrary spatial path. Despite the limitations of the PD control model, the basic approach of directly coupling the driver's steering actions to the state of a small set of plausible perceptual variables has strong intuitive appeal so it is valuable to examine the viability of this approach.

Steering Control Model 2: Pursuit of a Virtual Target

Our second model embodies a different approach to steering control, in which the driver pursues a target placed in the environment. For some steering tasks, the target, such as a salient location on the back of a car being followed, may be directly perceived. For tasks such as lane keeping and lane changing, the driver pursues a virtual target in the scene. In Boer's curve negotiation model (Boer, 1996), on which our target model is based, the driver continuously steers toward a target that is placed just inside the inner lane boundary of a curve, near the tangent point (the point where the line of sight is tangent to the inner lane boundary). Drivers often fixate on the tangent point during curve negotiation (Land and Lee, 1994). On the basis of an estimate of the distance and bearing to the target at each moment, the model steers the car toward the target. To accomplish this, the model first computes a curve of minimum constant curvature that passes from the driver through the target point. Assuming that the driver has an internal model of the relationship between steering angle and path curvature, this computed spatial trajectory is used to calculate a new steering angle. Over time, the target point continually advances around the curve in the case of curve negotiation or along the road in the case of lane keeping. The desired steering angle is recomputed frequently as the target advances. As long as the target remains a sufficient distance from the vehicle (an act that is accomplished through speed control), the model keeps the vehicle within the lane boundaries and maintains lateral acceleration within tolerable bounds. The model also incorporates driver limitations similar to those described for the PD control model.

Formulation of the target trajectory. The application of this model to the lane correction task requires the definition of an appropriate target to be tracked over time. In the initial development of the model, the target's location is defined in the 3-D world coordinate frame of the road. Other representations are also possible, however. The model uses the target's distance and bearing relative to the car to adjust steering at each moment. This information could be represented in the egocentric reference frame of the driver or could be expressed in terms of visual angles (Boer et al., 1998).

The lane correction task used in the experiments involves steering the car to center the driver on the midline. In this case, it is appropriate to assume that the target is located on the midline. The model can easily be extended to the real driving situation, in which the car is steered along a virtual center of the lane. With the target placed on the midline, there is a choice regarding its movement over time. Initial explorations with the model, aimed toward capturing the detailed shape of human steering profiles, showed that at the start of the lane correction, the target must remain at a fixed position on the midline to obtain a steering trajectory that turns the car sharply to head back toward the midline. Then, to generate a second sharp turn to realign the car with the road, it is necessary for the target to move along the midline with a speed that is less than the speed of the car so that the car is still closing in on the target. Finally, as the driver nears the completion of the task, the target must remain ahead of the car, moving at a speed at least as great as the speed of the car. This overall trajectory of the target point has several parameters: the initial fixed position, the two times at which it changes speed, and the two speeds.

Given this general form for the target trajectory, the experimental data were used to provide a quantitative description of trajectory parameters. At each moment, we considered the current position and heading of the car, constructed a circular path that would be followed if the current steering angle were maintained, and determined where this path intersected the midline. The movement of this intersection point along the midline can be used as an estimate of the trajectory of a virtual target being pursued by the driver. This construction essentially performs the reverse of the computation that the target model uses to determine a desired steering angle at each moment. It ignores the effect of driver limitations, such as a limit on the rate of change of steering, but this analysis indicates a good overall parameterization of the target trajectory required to reproduce human steering behavior.

We explored a variety of criteria that the driver may use to initiate the two transitions that occur on the target trajectories. Our aim was to find a criterion that is meaningful, easy to compute, and that results in a close match between model and driver performance with few coefficients. We found such a criterion based on the *time-to-lane-crossing* (TLC), defined here as the time it would take the car to reach the midline if it followed a straight path along its current heading at its current speed. Human driving studies suggest that TLC is used, for example, to assess when to perform error correction during lane keeping (Godthelp, 1988; Godthelp, Milgram, & Blaauw, 1984). Simulations with the model and data for Driver 1 revealed that the times at which the two transitions occur on the target trajectories are correlated well with times at which the car reaches two different critical values of TLC.

The final target model. In the final model, the driver continuously pursues a virtual target that has a three-phase movement trajectory in space, in which the target first stays at a fixed position for a short time, then slowly moves at a speed less than the speed of the car, and finally moves at a faster speed. The target trajectory is characterized by the following six coefficients.

m, b: The initial target position z_0 is a linear function of car speed v: $z_0 = mv + b$.

$t_{1,2}$: The critical TLC at which the target begins to move slowly, switching from Phase 1 to Phase 2.

s_2: The initial slow speed of the target during Phase 2, as a fraction of car speed.

$t_{2,3}$: The critical TLC at which the target changes speed, switching from Phase 2 to Phase 3.

s_3: The final, fast speed of the target during Phase 3, as a fraction of car speed.

On the basis of the above target trajectory and a known car model, a desired steering angle is computed at each moment. A final steering angle is then obtained, after imposing driver limitations. The same driver model that was used in the PD control model, consisting of a response delay of 0.4 s and a third-order linear filter, was incorporated in the target model. We formally identified the nine coefficients that characterize the target trajectory and driver model that produce lateral position and steering profiles that best fit the mean position and steering profiles for Drivers 1 and 3. Details of this derivation are given in Appendix B.

Simulations with the target model: Results and analysis. The performance of the target model suggests that the characterization of drivers' steering actions in terms of the pursuit of a target in the environment also results in steering behavior that is similar to that of human drivers. The computed steering profiles show the same dependencies of amplitude and timing on the visual conditions at the start of the lane correction. Figures 17 and 18 compare the model results and data for Drivers 1 and 3, respectively. The model coefficients are given in the legends. For reasons described in Appendix A, we again identified two sets of coefficients, with the first set using data from Experiments 1 and 2 and the second set using data from Experiment 3. The top row of Figures 17 and 18 shows lateral position as a function of time, whereas the middle row shows steering angle profiles. Solid curves correspond to human data, and dotted curves are model output. In the bottom row, the solid curves show the target trajectories generated by the model. The dotted curves in these figures show the position of the car along the road. The left, middle, and right columns of the figures show results for three different headings, speeds, and lateral positions, respectively. For different headings and lateral positions, the target trajectories are the same. The trajectories change with speed because the initial target position is parameterized by speed, and the speed of movement of the target during the second and third phases is expressed as a fraction of car speed.

Overall, there is a close fit between the model results and data for both drivers. In agreement with the data, steering amplitude increases with initial heading, with no change in timing. The temporal extent of the steering profiles decreases with increasing speed. The amplitude of the first peak of the model steering profiles does not vary with speed for Driver 1 and decreases slightly with increasing speed for Driver 3. These behaviors are also seen in the data. For both drivers, the amplitude of the model steering profiles increases with the initial lateral position. This dependency is seen in the data obtained for Driver 1 but not for Driver 3. In the model results for both drivers, there was no change in the timing of the steering action with changes in the initial lateral position. Similar to the PD control model, the target model generates steering actions that complete the task in roughly the same time for different headings and lateral positions. In all cases, the detailed shape of the steering and position profiles is captured well by the model. Unlike the PD control model, the shape of the steering profile during the final return of the steering wheel to its upright position is matched closely by the target model, and there are no oscillations in lateral position and steering after completion of the task. At this point, the car's heading and lateral position are aligned with the midline, and the target is moving along the midline directly ahead of the car.

Differences in behavior across the 2 drivers are reflected in changes in the model coefficients (note that the results in Figures 17 and 18 are displayed on different spatial and temporal scales). The lower amplitude, slower steering actions of Driver 3 are achieved in part by placing the target at a larger initial distance from the car. Over the range of speeds used in this analysis, the initial target position used in the model varies from 53–63 m for Driver 1 and 86–106 m for Driver 3. The target also begins to move sooner for Driver 1 (1.1–1.4 s over the range of speeds) than for Driver 3 (1.5–1.8 s). The combinations of driver model coefficients again also contribute to the different response rates of the 2 drivers.

The behavior of the target model can be explained directly in terms of the model coefficients. At each moment, the model computes a desired steering angle that drives the car along a

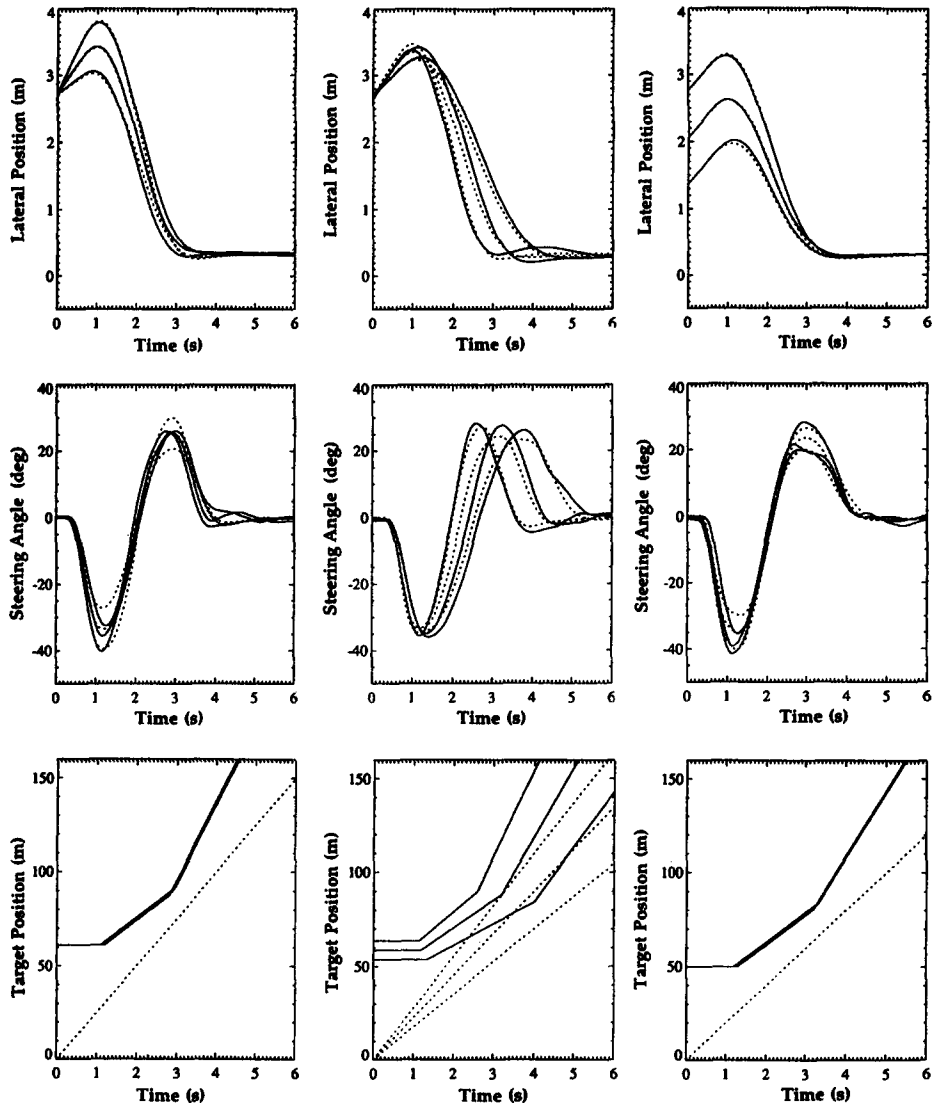

Figure 17. Comparison of the results of the target model with steering data for Driver 1. Top row: Lateral position as a function of time. Middle row: Steering angle profiles. Solid curves show human data from individual trials, and dotted curves show model output. Bottom row: Solid curves show the target trajectories generated by the model, with the position of the target on the midline plotted as a function of time. The dotted curves in these figures show the position of the car along the road. Results are shown for three of the different initial headings (1°, 2°, and 3°; left column), speeds (17.5, 22.5, and 27.5 m/s; middle column), and lateral positions (1.38, 2.08, and 2.78 m; right column) used in Experiments 1–3. Computed model coefficients using data from Experiments 1 and 2 were $\omega_n = 7.07$, $\zeta = 0.547$, $p = 6.331$, $b = 36.183$, $m = 0.995$, $t_{1,2} = 7.754$, $s_2 = 0.658$, $t_{2,3} = 0.237$, and $s_3 = 1.681$. Model coefficients using data from Experiment 3 were $\omega_n = 9.333$, $\zeta = 0.82$, $p = 7.893$, $b = 53.2523$, $m = -0.158$, $t_{1,2} = 6.766$, $s_2 = 0.803$, $t_{2,3} = 0.108$, and $s_3 = 1.75$.

minimum curvature circular path to the target. As target distance decreases or target bearing increases, a higher curvature path corresponding to a larger steering angle is needed to pursue the target. The maximum steering angle reached during the first phase of the steering trajectory and the initial rate of rotation of the steering wheel are determined by the initial, fixed target location (the coefficients m and b) and the driver's limitations (the initial time delay and third-order filter). The closer initial target distance obtained for Driver 1 results in a larger initial steering change. The combination of a larger initial heading or lateral position and a fixed, initial target position results in a larger target bearing and a larger amplitude of the first peak of the steering profile. The sharpness of this first peak is affected by the time at which the target begins to move (the coefficient $t_{1,2}$). If the target stays at a fixed location for a longer time, the steering profile will show a plateau at a fixed steering angle that keeps the car on a circular path toward the fixed target. The extended plateau seen in the data for Driver 4 in Figures 2 and 3 can be interpreted as the pursuit of

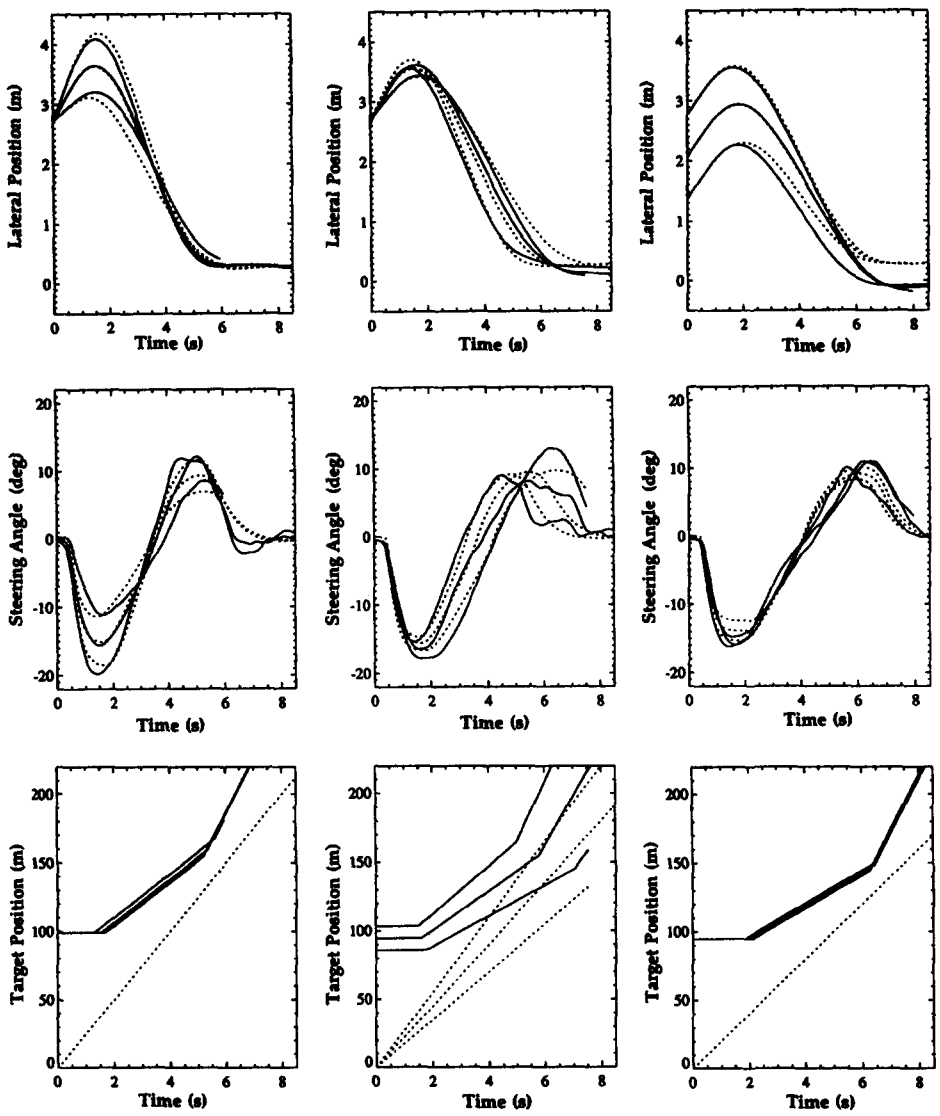

Figure 18. Comparison of the results of the target model with steering data for Driver 3. Top row: Lateral position as a function of time. Middle row: Steering angle profiles. Solid curves show human data from individual trials, and dotted curves show model output. Bottom row: Solid curves show the target trajectories generated by the model, with the position of the target on the midline plotted as a function of time. The dotted curves in these figures show the position of the car along the road. Results are shown for three of the different initial headings (1°, 2°, and 3°; left column), speeds (17.5, 22.5, and 27.5 m/s; middle column), and lateral positions (1.38, 2.08, and 2.78 m; right column). Computed model coefficients using data from Experiments 1 and 2 were $\omega_n = 10.095$, $\zeta = 1.202$, $p = 11.950$, $b = 54.852$, $m = 1.770$, $t_{1,2} = 506.677$, $s_2 = 0.634$, $t_{2,3} = 0.343$, and $s_3 = 1.790$. Model coefficients using data from Experiment 3 were $\omega_n = 6.875$, $\zeta = 0.967$, $p = 17.337$, $b = 93.978$, $m = 0.037$, $t_{1,2} = 43.521$, $s_2 = 0.605$, $t_{2,3} = 0.302$, and $s_3 = 2.112$.

a target that stays at a fixed location for 2–3 s. When the target begins to move, the steering wheel is rotated back through its upright position, and the rotation rate of the wheel depends on the speed of the target relative to the car (the coefficient s_2). A higher target speed results in a more rapid wheel rotation. The amplitude and sharpness of the second peak of the steering profile and the shape of the final return of the wheel to its upright position are determined by the time at which the target changes to a higher speed (the coefficient $t_{2,3}$) and its final speed relative to the car (the coefficient s_3). If this final transition is delayed, then the car will move closer to the target (because of its slower speed during the middle phase of the target trajectory), and the smaller target distance will result in a higher curvature path and larger desired steering angle. If the final transition occurs earlier and the final target speed is large, the steering wheel will be turned back less rapidly to its upright position, to pursue a more distant target (this would give final steering profiles similar to those obtained by the PD control model). In general, the behavior of the target model is

more intuitive than that of the PD control model and can be explained more directly in terms of the model coefficients.

Steering control during visual occlusion. To steer the car through occlusions, target movement must be extrapolated during these times. In the implementation used to generate the results shown in Figures 17 and 18, target location was defined in a fixed-world coordinate frame, and the 3-D positions of the target and car were used to calculate target distance and bearing. We conducted simulations with the model using this same representation to extrapolate the target movement during occlusion and introduced the same noise sources that were used to test the PD control model under occlusion. Figure 19 shows the results of this modified target model, in which we simulated performance during a 4-s occlusion. The results are shown in the same format as Figure 16. The lateral-position error and the amplitude of subsequent steering corrections that occur when vision returns are similar to that observed for Driver 1 (see Figure 11A and 11B). For shorter occlusions, this model also yields behavior comparable to that of Driver 1. This analysis suggests that given reasonable assumptions about sources of error, an extrapolation of the target movement may be sufficient to maintain adequate steering control for short occlusion periods.

The development of the target model thus far has used a fixed-world coordinate frame to represent target location. The critical

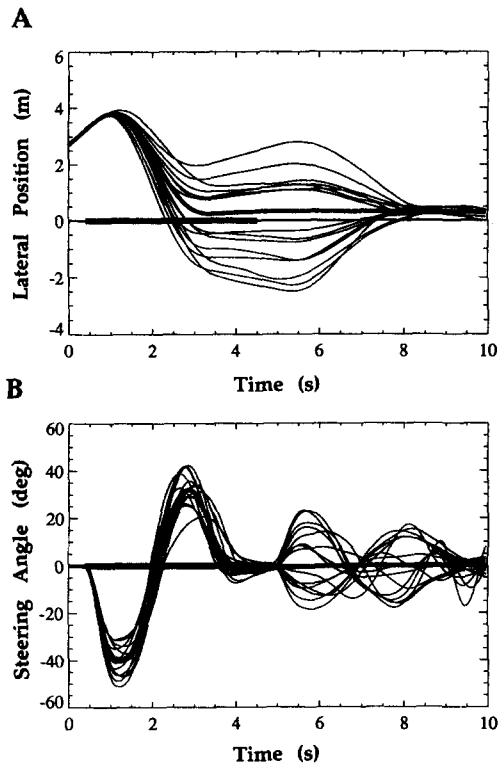

Figure 19. Results of the target model during visual occlusion. Lateral position profiles (Panel A) and steering angle profiles (Panel B), obtained with added noise sources and extrapolation of the target movement during occlusion. Thick line shows the results obtained under visual feedback with no noise, and thin lines show the results of 15 trials obtained with a 4-s occlusion period. The occlusion period is highlighted on horizontal axes of graphs by a bold line.

information derived at each moment is the distance and bearing to the target. In principle, this information could be maintained and extrapolated during occlusion in the egocentric reference frame of the driver. Given our description of the target trajectory, egocentric target distance D_T decreases linearly during the first two phases of the trajectory and increases linearly during the third phase. Given an initial estimate of D_T derived from perceptual information at the start of the lane correction, one can then extrapolate linearly the change in D_T over time. The transition between decreasing and increasing target distance could occur when D_T reaches a critical value (in spatial or temporal terms). In the case of target bearing, when D_T is large relative to the lateral position of the car, the change in target bearing at each moment depends largely on the change in heading. If drivers have an internal model of how the current speed and steering angle affect the change in heading of the car over time, then in principle, they could predict the heading change that results from their steering actions. Drivers can then use this predicted heading change to estimate the change in target bearing over time. Thus, in principle, the target could be defined in an egocentric coordinate frame that could facilitate the extrapolation of target movement through brief occlusions (Boer et al., 1998).

Summary of the target model. The goal of steering in the target model is to pursue a continually advancing target placed in the environment. In our formulation of this model for lane corrections, human data were used to specify a three-phase target trajectory that resulted in a close fit between the steering and lateral position profiles generated by the model and observed in the data. Some aspects of human steering profiles, such as the final return of the steering wheel to its upright position at the end of the maneuver, were fit more closely by the target model than the PD control model. The changes in behavior of the target model for different initial conditions of the lane correction can be explained directly in terms of the model coefficients that describe the target trajectory. Differences between drivers can also be explained easily by differences in model coefficients. Thus the target model offers a clear framework in which the experimental observations can be summarized and explained.

One of the most appealing aspects of this approach is its adaptability to a range of steering tasks. To apply this model to a particular task, one needs only to define an appropriate target to pursue. Many steering tasks have natural targets. In lane keeping or lane changing, the driver can pursue a virtual target that moves along the center of the current or adjacent lane. For curve negotiation, the tangent point on the inner lane boundary can serve as the target (Boer, 1996). During car following, the driver could pursue a salient location on the back of the lead car. To create a situation in which a driver could negotiate around an obstacle, one could place a target point on one side of the obstacle. Once the target is defined, the same control algorithm can then be applied for each task. The driver can seamlessly shift from one steering task to another simply by redirecting the target in a way that is appropriate to the current steering goal. This leads to a unified framework for performing multiple steering tasks, which may need to be performed simultaneously (e.g., changing lanes while negotiating a curve).

Finally, the simplicity of the target information needed to control steering facilitates the continuation of control during occlusion. With reasonable assumptions about error sources, the con-

tinuous extrapolation of target information may be adequate to cope with brief occlusions. We raised the possibility that target distance and bearing could be represented and extrapolated directly in an egocentric reference frame. Similar to the PD control model, this approach assumes that the driver has an internal model of how steering changes and speed affect the rotation of the car. An extrapolation mechanism of this sort circumvents the need to plan and to represent internally an extended steering trajectory or spatial path to reach the target.

Summary and Conclusions

We examined driver performance of a lane correction task in which the visual information at the outset of the maneuver was systematically varied. The data reveal the dependence of steering behavior on specific visual cues. Across all drivers, steering amplitude increased with increasing heading of the car at the start of the maneuver, and the temporal extent of steering actions decreased with increasing speed. There was no consistent effect of lateral position on immediate steering actions. These dependencies prevailed during a brief period of visual occlusion of 1.5 s that began shortly after the start of the maneuver. With longer occlusion times, most drivers showed a significant increase in the variability of their steering. There were large differences between drivers in the amplitude and timing of steering actions in all conditions, but all drivers showed the same basic adjustments of behavior with the initial visual conditions.

To explain how this steering behavior may arise, we developed two models that embody fundamentally different approaches to steering control and account for driver behavior in different ways. In the PD control model, steering adjustments are made in response to perceived deviations of the current vehicle state from a desired state. The state is characterized by lateral position and its first and second temporal derivatives (or, equivalently, lateral position, heading, and the first temporal derivatives of these two variables). In the target model, steering adjustments are made in response to the distance and bearing to a virtual target that follows a specified movement along the midline. One can think of the target as effectively pulling the vehicle through the environment.

We showed how both models can be formulated to produce behavior similar to that of human drivers for the task used in this study. It is important to stress that the unconstrained nature of the task made it essential to consider human data closely when formulating the models. The choice of perceptual variables used in the PD control model and the characterization of the target trajectory used in the target model are not dictated by the task requirements alone. Once the basic structure of the models was specified, the human data were used to compute model coefficients that yield behavior that most closely matches that of human drivers.

Both models exhibit the same dependencies of steering amplitude and timing on the initial conditions of the lane correction observed in the data. Both models also reproduce much of the detailed shape of human steering profiles and the variations in these profiles across drivers. Thus, both may be considered viable models of human steering control. With the target model, however, we can more clearly explain the underlying basis for human steering behavior because of the direct and intuitive relationship between the description of the target movement and the driver's response. We also argue that the target model may be more easily adapted to other steering tasks because of the existence of natural targets to pursue in other contexts.

We briefly explored an approach to continuing control through occlusion, on the basis of extrapolating the information that is used to compute the desired steering angle at each moment. This approach assumes that the driver has an internal model of how steering actions alter the state of the car. Simulation results with both models suggest that this strategy may be adequate for maintaining control for short occlusion periods of 1–2 s. Given a particular combination of error sources, we showed how both models produce results that show a similar degradation in performance with longer occlusion periods as seen in the human data.

Any viable model for continuing control during occlusion must be able to assume control at any moment and for arbitrary durations. A reduction of visual input in the direction ahead of the car can occur when the driver makes a voluntary eye movement (e.g., looks over his or her shoulder to prepare for a lane change). In these situations, the driver can anticipate the occlusion and plan an extended steering action to maintain control during the shift of gaze. Other situations arise that the driver cannot anticipate. The sudden appearance of an obstacle approaching the driver's path can unexpectedly draw the driver's attention and gaze away from the road. These spontaneous events can occur at any moment and must also be accommodated by the steering control model. An advantage of an extrapolation strategy is that it can continue control for short time periods without the need for planning an extended steering action. This facilitates the continuation of control as the driver's attention is shifted between multiple tasks during driving.

From an empirical standpoint, it would be useful to explore whether the observations here can be confirmed in natural driving conditions. Our task forced the driver to initiate a corrective maneuver at a particular time. Normally, drivers choose when to make corrections on the basis of factors such as perceived error relative to a desired state or perceived TLC (Godthelp, 1988; Godthelp et al., 1984). In the study by Godthelp (1988), drivers were engaged in lane keeping on a straight road and were asked to ignore their path error and to not perform any steering corrections until the car reached the final moment when they could still comfortably correct the car's state to prevent crossing a lane boundary. Drivers consistently waited until the TLC was about 1.5 s before making a correction. This suggests that TLC is important for deciding when to make a correction, but our study suggests that it does not directly influence quantitative aspects of the steering correction itself. It would be useful to examine driving data obtained during normal lane keeping to determine when corrections are made and whether the actual steering corrections initiated voluntarily by the driver show the same dependence of amplitude and timing on the initial visual conditions.

In our task, visual input was removed abruptly and completely during the occlusion period. It would be interesting to explore whether similar behavior results when drivers still have some visual feedback but have their attention drawn away from the steering task for short periods of time to perform a secondary task. Levison and Cramer (1995; Levison, 1979) propose a model for the integration of multiple tasks during driving, in which attentional resources are allocated to different tasks depending on the

perceived penalty of not performing each task at a given moment. When attention is shifted to a nonvisual task while preserving visual input from the direction ahead of the car, it is assumed that there is an increase in the noise associated with the measurement of perceptual variables related to the steering task.

Our work also contributes to the broader study of visuomotor integration. Over the past decade, an approach to visuomotor integration in biological and robotic systems has evolved, in which actions are directly coupled to sensory input, with no intervening internal model of the environment that is used to plan appropriate actions (Aloimonos, 1992; Brooks, 1991a, 1991b; Duchon, Warren, & Kaelbling, 1998; Warren, 1988). One focus of this research has been to identify simple and direct mappings between specific motor tasks and the critical visual information needed to perform the task adequately. Examples of this approach include (a) a model of braking during driving based on the regulation of tau, which is the rate of change of the time-to-collision with an object (Lee, 1976; Yilmaz & Warren, 1995); (b) a model of steering through a corridor based on maintaining equal optical flow in the left and right halves of the visual field (Duchon et al., 1998); and (c) detection of approaching obstacles by monitoring flow field divergence (Aloimonos, 1992).

Both of the models presented here are in the spirit of this general approach to visuomotor integration. We propose that steering is coupled directly to specific variables. In the case of the PD control model, these variables can include lateral position, heading, and their temporal derivatives. Information about lateral position can be derived from splay angle, which can be measured directly from the image, and heading can be computed from optical flow. Both quantities can be derived without constructing an explicit 3-D representation of the environment. Similarly, the distance and bearing to a target being pursued by the target model can be derived on the basis of image or optical flow cues, without the need for an explicit model of the 3-D structure of the environment. Although it is possible for both models to derive their input from an internal 3-D representation of the world, it is not necessary. Our work therefore reinforces the viability of the general approach of coupling motor actions directly to relevant visual cues.

The experimental paradigm that we developed here provides a valuable tool for exploring the specific visual cues used to guide motor actions. Our occlusion paradigm allowed us to carefully control the visual conditions present at the start of a motor response and to examine quantitative aspects of the specific action made in response to those conditions. Under occlusion, the steering trajectory that was first initiated by the driver was not further adjusted as a result of changing visual conditions, allowing us to examine how visual input is used to initiate an appropriate, extended motor response. Brief occlusion of relevant visual information for performing a motor task is a common occurrence, and the control strategies that the human system has adopted have evolved in part to cope effectively with momentary losses of visual input. Our experimental paradigm allowed us to quantify the limits of performance of the human system under these conditions. Finally, the formulation of specific models of steering control whose design is closely guided by human data provided a framework for explaining the connections that we observed between the drivers' sensory input and subsequent actions.

References

Aloimonos, Y. (1992). Is visual reconstruction necessary? Obstacle avoidance without passive ranging. *Journal of Robotic Systems, 9,* 843–858.

Beall, A. C., & Loomis, J. M. (1997). Optical flow and visual analysis of the base-to-final turn. *International Journal of Aviation Psychology, 7,* 201–223.

Beusmans, J., & Rensink, R. (Eds.). (1995). *Cambridge basic research 1995 annual report* (Rep. No. CBR TR 95-7). Cambridge, MA: Cambridge Basic Research.

Boer, E. R. (1996). Tangent point oriented curve negotiation. *Proceedings of the 1996 IEEE Intelligent Vehicles Symposium,* 7–12.

Boer, E. R., Hildreth, E. C., & Goodrich, M. A. (1998). Drivers in pursuit of perceptual and virtual targets. *Proceedings of the 1998 IEEE International Conference on Intelligent Vehicles, 1,* 291–296.

Brooks, R. A. (1991a). Intelligence without representation. *Artificial Intelligence, 47,* 139–160.

Brooks, R. A. (1991b, September 13). New approaches to robotics. *Science, 253,* 1227–1232.

Cavallo, V., Brun-Dei, M., Laya, O., & Neboit, M. (1988). Perception and anticipation in negotiating curves: The role of driving experience. In A. G. Gale, M. H. Freeman, C. M. Haslegrave, P. Smith, & S. P. Taylor (Eds.), *Vision in vehicles II* (pp. 365–374). Amsterdam: Elsevier Science.

Crowell, J. A., & Banks, M. S. (1993). Perceiving heading with different retinal regions and types of optic flow. *Perception & Psychophysics, 53,* 325–337.

Donges, E. (1978). A two-level model of driver steering behavior. *Human Factors, 20,* 691–707.

Dorf, R. C., & Bishop, R. H. (1995). *Modern control systems.* Reading, MA: Addison-Wesley.

Duchon, A. P., Warren, W. H., & Kaelbling, L. P. (1998). Ecological robotics. *Adaptive Behavior, 6,* 471–505.

Evans, L. (1991). *Traffic safety and the driver.* New York: Van Nostrand Reinhold.

Godthelp, J. (1985). Precognitive control: Open- and closed-loop steering in a lane-change manoeuvre. *Ergonomics, 28,* 1419–1438.

Godthelp, H. (1986). Vehicle control during curve driving. *Human Factors, 28,* 211–221.

Godthelp, H. (1988). The limits of path error-neglecting in straight lane driving. *Ergonomics, 31,* 609–619.

Godthelp, H., Milgram, P., & Blaauw, G. J. (1984). The development of a time-related measure to describe driving strategy. *Human Factors, 26,* 257–268.

Groen, F. C. A., Hirose, S., & Thorpe, C. E. (Eds.). (1993). *Intelligent autonomous systems.* Washington, DC: IOS Press.

Hess, R. A., & Modjtahedzadeh, A. (1990, August). A control theoretic model of driver steering behavior. *IEEE Control Systems Magazine, 10,* 3–8.

Iyengar, S. S., & Elfes, A. (1991). *Autonomous mobile robots: Control, planning and architecture.* Los Alamitos, CA: IEEE Computer Society Press.

Kanade, T., Groen, F. C. A., & Herzberger, L. O. (Eds.). (1989). *Intelligent autonomous systems 2.* Amsterdam: Stichting International Congress of Intelligent Autonomous Systems.

Land, M. F., & Lee, D. N. (1994, June 30). Where we look when we steer. *Nature, 369,* 742–744.

Lee, D. N. (1976). A theory of visual control of braking based on information about time-to-collision. *Perception, 5,* 437–459.

Levison, W. H. (1979). A model for mental workload in tasks requiring continuous information processing. In N. Moray (Ed.), *Mental workload: Its theory and measurement.* New York: Plenum Press.

Levison, W. H., & Cramer, N. L. (1995). *Description of the integrated driver model* (Tech. Rep. No. 7840). Cambridge, MA: Bolt, Berenak, & Newman Systems & Technologies.

Lewis, F. L., & Syrmos, V. L. (1995). *Optimal control.* New York: Wiley.

Luenberger, D. G. (1973). *Introduction to linear and nonlinear programming.* Reading, MA: Addison-Wesley.

Masaki, I. (Ed.). (1992). *Vision-based vehicle guidance.* New York: Springer-Verlag.

McRuer, D. T., Allen, R. W., Weir, D. H., & Klein, R. H. (1977). New results in driver steering control models. *Human Factors, 19,* 381–397.

McRuer, D. T., & Weir, D. H. (1969). Theory of manual vehicular control. *Ergonomics, 12,* 599–633.

Modjtahedzadeh, A., & Hess, R. A. (1993). A model of driver steering control behavior for use in assessing vehicle handling qualities. *Journal of Dynamic Systems, Measurement, and Control, 15,* 456–464.

Ogata, K. (1990). *Modern control engineering* (2nd ed.). Englewood Cliffs, NJ: Prentice Hall.

Reid, L. D., Solowka, E. N., & Billing, A. M. (1981). A systematic study of driver steering behavior. *Ergonomics, 24,* 447–462.

Riemersma, J. B. J. (1981). Visual control during straight road driving. *Acta Psychologica, 48,* 215–225.

Sheridan, T. B., & Ferrell, W. R. (1981). *Man-machine systems, information, control, and decision models of human performance.* Cambridge, MA: The MIT Press.

Thorpe, C. E. (1990). *Vision and navigation: The Carnegie Mellon Navlab.* Boston: Kluwer.

van den Berg, A. V. (1992). Robustness of perception of heading from optic flow. *Vision Research, 32,* 1285–1296.

Warren, W. H. (1988). Action modes and laws of control for the visual guidance of action. In O. G. Meijer & H. Roth (Eds.), *Complex movement behavior: The motor-action controversy.* Amsterdam: Elsevier Science/North-Holland.

Warren, W. H., & Hannon, D. J. (1990). Eye movements and optical flow. *Journal of the Optical Society of America A, 7,* 160–169.

Yilmaz, E., & Warren, W. H. (1995). Visual control of braking: A test of the $\dot{\tau}$ hypothesis. *Journal of Experimental Psychology: Human Perception and Performance, 21,* 996–1014.

Appendix A

The Implementation of the PD Control Model

The implementation of the PD control model used Equation 3 (described in the text) to compute a desired yaw rate at each moment, Y_d, from which a desired steering angle, θ_s, was then computed. For the driving simulator used in this study, the car model is based on a three-wheel car with a 3-m wheel base. The radius of the car's instantaneous trajectory, R_c, is related to Y_d as follows: $R_c = v/Y_d$. The radius R_c is then related to the car wheel angle, θ_c, through the following equation: $R_c = 3/\tan(\theta_c)$. Finally, θ_c is related to the steering angle θ_s by $\theta_c = 0.00423 \times \theta_s^{1.3}$. It is assumed that the driver has an internal model of this transformation.

A third-order digital filter was used to model driver limitations. In the continuous frequency or s-domain the transfer function is

$$U(s) = [\omega_n^2 p/(s + 2\zeta\omega_n s + \omega_n^2)(s + p)]C(s),$$

where ω_n is the frequency at which the filter would oscillate if it were undamped and is directly coupled to the rate of change in steering angle. ζ is the damping factor, which when greater than one, eliminates oscillations, and p affects the maximum overshoot and settling time such that a smaller value causes the system to reach the desired input later and overshoots it less (see Ogata, 1990). The combination of these three parameters is captured in $\beta = p/\zeta\omega_n$, which results in a slower response for small values (i.e., $\beta < 1$) and a fast response for larger values.

The nine model coefficients (i.e., six coefficients from Equation 3 and three from the driver model) that result in the best match between the model output and the data from Drivers 1 and 3 were identified, using mean steering and lateral position profiles for 15 initial conditions. The mean profiles were computed by averaging data from 10 individual trials for each of the five heading, speed, and lateral positions used in Experiments 1, 2, and 3. The heading trials were chosen from the data obtained with a speed of 25 m/s. The use of mean data results in an estimate of the driver's desired, noise-free response. (We also identified the coefficients using a subset of the raw data trials, but the mean data produced better results.)

The error function used in the optimization combined the fit between both the steering and lateral position data and model results. In particular, the following error function was minimized:

$$\text{error} = \delta\_\text{error} + 3 \times \theta_s\_\text{error},$$

where δ_error is the total absolute error in lateral position, measured in meters, and θ_s_error is the total absolute error in steering angle, measured in radians. Using Equation 3, together with the car and driver models, a new steering angle was computed every 50 ms and used to update the 3-D position of the car. For direct comparison, the human data were interpolated and resampled at 50-ms intervals. The error at each time step was summed over a time period that extended 0.5 s beyond the approximate time of completion of the steering maneuver. This temporal extent varied with speed and also varied across the 2 drivers. The total time used in this analysis ranged between the first 4 s and first 6 s of data for Driver 1 and ranged between the first 6 s and first 8 s of data for Driver 3 (the exact time depended on speed). The relative weight of the lateral position and steering angle error terms was chosen to produce the best match between model predictions and human data. The Simplex method (Luenberger, 1973) was used to perform the optimization.

In the case of Driver 1, all of the data from Experiment 3, in which the lateral position at the start of the lane correction was varied, exhibited more rapid steering actions. One of the conditions of this experiment overlaps with one of the conditions of Experiment 2; for this same condition, the average time of the zero-crossing was about 200 ms earlier in the steering profiles obtained in Experiment 3. The data from Experiments 1–3 were collected on different days over a 2-week period, which could have resulted in such shifts in behavior. If the data from all three experiments are considered together to compute the model coefficients, this discrepancy in timing significantly degrades the quality of the fit between the model and human data. As a consequence, two sets of coefficients were identified for Driver 1. The first set used data from Experiments 1 and 2 (varying the initial heading and speed), and the second set used data from Experiment 3 (varying the lateral position at the start of the lane correction).

(Appendixes continue)

In the case of Driver 3, all of the data from Experiment 3 exhibited large overshoots of the midline by an average of about 0.5 m. This was not seen for the overlapping condition in Experiment 2. If the data of Driver 3 from all three experiments are considered together when computing the model coefficients, the consistent presence of this overshoot in part of the data also degrades the quality of fit between the model and human data. As a consequence, we also identified two sets of coefficients for Driver 3. As in the case of Driver 1, the first set used data from Experiments 1 and 2, and the second set used data from Experimemt 3.

Appendix B

Implementation of the Target Model

The implementation of the target model used the same car and driver models described in Appendix A. Values for the six coefficients characterizing the target trajectory (m, b, $t_{1,2}$, s_2, $t_{2,3}$, and s_3) described in the text and the three coefficients (ω_n, ζ, and p) characterizing the driver limitations were identified by maximizing the fit of the model results to data for Drivers 1 and 3. The identification used the same mean steering and lateral-position profiles that were used for identification of the coefficients for the PD control model. The optimization also used the same error function, based on a combination of lateral position and steering error, summed over the same temporal extents as described in Appendix A. The analysis used data that extended about 1 s beyond completion of the task (0.5 s longer than the temporal extents used to identify the PD control model coefficients). We identified two sets of coefficients for each driver, with the first set derived from the data for Experiments 1 and 2 (varying the initial heading and speed) and with the second set derived from the data for Experiment 3 (varying the initial lateral position). Again, Simplex search was used to perform the optimization.

To generate the extended steering and position profiles from the target model, we initially represented both the target location and the current location of the car in a fixed 3-D coordinate frame. The relative positions of the target and car were used to compute the current target distance and bearing, which were then used to compute the minimum curvature circular path from the car to the target. Given the car model described in Appendix A, we then used this path curvature to compute the desired steering angle. The temporal filter described above was then applied to compute the final steering angle.

Received September 12, 1996
Revision received August 13, 1998
Accepted June 23, 1999 ■